**Thesis**

# Oncolytic Adenovirus Utilizing RNA Stabilization Mechanism Can Synergize with Chemotherapy

# RNA 安定化メカニズムを応用した腫瘍溶解性アデノウイルスとそのがん化学治療法との相乗効果

**September 2020**

**Hokkaido University**

**Hossain Elora**

**Thesis**

# Oncolytic Adenovirus Utilizing RNA Stabilization Mechanism Can Synergize with Chemotherapy

# RNA 安定化メカニズムを応用した腫瘍溶解性アデノウイルスとそのがん化学治療法との相乗効果

**September 2020**

**Hokkaido University**

**Hossain Elora**

**Table of content**


| **Topic** | **Page no** |
|---|---|
| Basic/reference paper list | 1 |
| List of presentations | 4 |
| **Chapter I** | 5 |
| 1.Intorduction | 6 |
| 1.2. The conventional method of cancer treatment | 6 |
| 1.3. Gene Therapy | 7 |
| 1.4. Oncolytic virotherapy | 7 |
| 1.5. Oncolytic Adenovirus | 10 |
| 1.6. Engineering oncolytic adenovirus by inserting ARE in the 3' untranslated region | 12 |
| 1.6.1. Construction of Ad-*fos*ARE | 12 |
| 1.6.2. What makes Ad-*fos*ARE is cancer-selective? | 13 |
| 1.7. Hypothesis | 16 |
| 1.8. Objectives | 17 |
| **Chapter II** | 20 |
| 2.1. Introduction | 21 |
| 2.2. Material and Method: | 22 |
| 2.3 Results | 27 |
| 2.3.1.Cancer-Selective replication of Ad-*fos*ARE in cancer cells | 27 |
| 2.3.2. HuR-mediated mRNA stabilization is essential for adenovirus replication | 29 |
| 2.3.3. In vitro cytolytic potentiality of Ad-*fos*ARE | 32 |
| 2.3.4. Comparison of the oncolytic effects of Ad-*fos*ARE and dl1520 | 36 |
| 2.4. Discussion | 38 |
| **Chapter III** | 39 |

| | |
|---|---|
| 3.1. Introduction | 40 |
| 3.2. Materials and method | 41 |
| 3.3. Results | 45 |
| 3.3.1. The potentiality of paclitaxel for synergism | 45 |
| 3.3.2. Synergistic effect of oncolytic adenovirus and paclitaxel. | 48 |
| 3.3.3. Effects of paclitaxel on Ad-*fos*ARE viral protein synthesis and mRNA stabilization | 50 |
| 3.3.4. Combination treatment Increases the Level of Posttranslationally Modified Tubulin | 52 |
| 3.3.5 Virus exit assay | 52 |
| 3.3.6. Effects of paclitaxel on the cell lysis activity of the virus | 54 |
| 3.3.7. *In vivo* synergistic effect of Ad-*fos*ARE and Paclitaxel in murine flank tumor | 55 |
| 3.3.8. PTX induces in vivo virus propagation. | 56 |
| 3.4. Discussion | 58 |
| 4. Future prospects and Conclusion | 60 |
| Acknowledgement | 61 |
| References | 62 |
| Supplementary data | 70 |

**List of Table**


| Topic | Page |
|---|---|
| Table 1.1: Oncolytic viruses used as an anti-cancer drug | 8 |
| Table 1.2: Current status of oncolytic virotherapy in Japan. | 9 |
| Table 1.3: List of acronyms | 18 |
| Table 2.1: Cell lines | 22 |
| Table 2.2: Antibodies used in this study. | 23 |


**List of Figures**


| Topic | Page |
|---|---|
| **Chapter I** | |
| Figure 1.1 Cancer-selective replication of oncolytic virus | 8 |
| Figure 1.2. Structure of Ad-*fos*ARE virus | 12 |
| Figure 1.3. Adenosine- and uridine-rich elements (ARE) | 13 |
| Figure 1.4. Degradetion and Stabilization of ARE mRNA. | 14 |
| Figure 1.5. HuR and stabilization of mRNA | 15 |
| Figure 1.6. Cancer selective replication of Ad-*fos*ARE | 16 |
| **Chapter II** | |
| Figure 2.1. Expression of early and late virus protein in Ad-*fos*ARE | 27 |
| Figure 2.2. The production efficiency and selectivity of Ad-*fos*ARE. | 28 |
| Figure 2.3. HuR relocalization in Ad-*fos*ARE infected cells and mRNA stabilization | 30 |
| Figure 2.4. Effect of HuR knockdown on virus replication. | 32 |
| Figure 2.5. Cell lysis activity of Ad-*fos*ARE | 33 |
| Figure 2.6. Cytopathic activity of Ad-*fos*ARE | 34 |
| Figure 2.7. Assessment of cell death by apoptosis | 35 |
| Figure 2.8. Comparison of the virus production and cell lysis activity of Ad-*fos*ARE with dl1520 and WT300. | 37 |
| **Chapter III** | |
| Figure 3.1. Effects of paclitaxel on cytoplasmic HuR exportation. | 46 |

| | |
|---|---|
| Figure 3.2. Western blot analysis of expression of coxsackie-adenovirus receptor (CAR) at different time-points. | 47 |
| Figure 3.3. To assess the viral replication and cell lysis activity of combination treatment Ad-*fos*ARE and PTX. | 49 |
| Figure 3.4. Effects of paclitaxel on Ad-*fos*ARE replication. | 50 |
| Figure 3.5. Expression of E1AmRNA and stabilization of E1a mRNA after combination treatment. | 51 |
| Figure 3.6. Effects of MTs stabilization on viral replication and viral exit. | 53 |
| Figure 3.7. Assessment of cell lysis activity of combination treatment. | 54 |
| Figure 3.8. *In vivo* tumor lysis potential of the combination therapy of Ad-fosARE and PTX in human cervical cancer xenograft nude mice. | 55 |
| Figure 3.9. Effect of PTX on Ad-*fos*ARE propagation in vivo. | 56 |
| Figure 3.10. Diagrammatic summary of the study | 60 |
| **Supplementary data** | 70 |
| Figure S.1. Time course of expression of virus protein in Ad-*fos*ARE infected cells. | 71 |
| Figure S.2. Calculation of combination index for Ad-*fos*ARE and PTX. | 72 |
| Figure S.3. E1A mRNA expression in Ad-*fos*ARE treated cells. | 73 |
| Figure S.4. Level of posttranslationally modified MTs after combination treatment. | 74 |
| Figure S.5. Intracellular virus propagation after combination treatment. | 75 |

# Basic/Reference Paper List

1. Basic papers: 1

Number of titles: 1

(1) Title:
**Advantages of Using Paclitaxel in Combination with Oncolytic Adenovirus Utilizing RNA Destabilization Mechanism**

(2) Author(s): **Elora Hossain,** Umma Habiba, Aya Yanagawa-Matsuda, Arefin Alam, Ishraque Ahmed, Mohammad Towfik Alam, Motoaki Yasuda and Fumihiro Higashino

(3) Academic journal in which the basic paper has been published :
*Cancers* **2020**, *12*(5), 1210; https://doi.org/10.3390/cancers12051210

(4) Month/year of publication May 2020

(5) Impact factor: **6.162**

2. Reference papers

Equally contributed first author

Number of titles: 1

(1) Title:
**Conditionally Replicative Adenovirus Controlled by the Stabilization System of AU-rich Elements-Containing mRNA**

**(2)** Author(s):
† **Equally contributed first author**

Yohei Mikawa†, Mohammad Towfik Alam†, **Elora Hossain**†, Aya Yanagawa-Matsuda, Tetsuya Kitamura, Motoaki Yasuda, Umma Habiba, Ishraque Ahmed, Yoshimasa Kitagawa, Masanobu Shindoh and Fumihiro Higashino

(3) Academic journal in which the basic paper has been published :
*Cancers* **2020**, *12*(5), 1205; https://doi.org/10.3390/cancers12051205

(4) Month/year of publication May 2020

(5) Impact factor: **6.162**

Number of titles: 2

(1) Title
**Enhanced oncolytic activity of E4orf6-deficient adenovirus by facilitating nuclear export of HuR**

(2) Author(s)
Ishraque Ahmed , Mohammad Towfik Alam b, Aya Yanagawa-Matsuda , **Elora Hossain**, Tetsuya Kitamura , Kazuyuki Minowa and Fumihiro Higashino

(3) Academic journal in which the basic paper has been published:
*BBRC*, 2020, 529(2);494-499 https://doi.org/10.1016/j.bbrc.2020.04.147

(4) Month/year of publication: July, 2020

5) Impact factor: **2.704**

Number of titles: 3

(1) Title
**Cisplatin enhances the oncolytic activity of E4orf6 deleted adenovirus through HuR relocalization**

(2) Author(s)
Umma Habiba, **Elora Hossain**, Aya Yanagawa-Matsuda, Abu Faem Mohammad Almas Chowdhur[5], Masumi Tsuda, Asad-uz- Zaman, Shinya Tanaka, Fumihiro Higashino

(3) Academic journal in which the basic paper has been published
*Cancers* **2020**, *12*(4), 809; https://doi.org/10.3390/cancers12040809

(4) Month/year of publication: May 2020

5) Impact factor: **6.162**

Number of titles: 4

(1) Title
**HuR translocation to the cytoplasm of cancer cells in actin-independent manner**

(2) Author(s)
Umma Habiba, Takeshi Kuroshima, Aya Yanagawa-Matsuda, Tetsuya Kitamura,
AFMA Chowdhury, Jumond P. Jehung, Elora Hossain, Hidehiko Sano, Yoshimasa Kitagawa, Masanobu Shindoh, Fumihiro Higashino

(3) Academic journal in which the basic paper has been published
Experimental Cell Research 369 (2018) 218–225

(4) Month/year of publication: May 2018

5) Impact factor: **3.246**

06/12/2020

Ph.D. candidate: Hossain Elora

**List of presentations**

Part of this study was presented in the following academic conferences:

**Oral Presentation:**

1. **Hossain E**, Habiba U, Matsuda AY, Kitamura T, and Higashino F. Microtubule stabilizer can enhance the activity of Oncolytic virus.
   The 5th Hokkaido University cross-department symposium. O-12. Sapporo, Japan, November 6th 2019.
2. **Hossain E**, Habiba U, Kitamura T, Matsuda AY, Higashino F, Efficacy of Ad+AU virus. Umea University and Hokkaido University exchange program. Sapporo, November 20th, 2019.

**Poster Presentation:**

3. **Hossain E**, Habiba U, Matsuda AY, Kitamura T, Higashino F. Evaluation of the efficacy of newly developed oncolytic adenovirus.
   The 108th JSP annual meeting. Tokyo International Forum department. P-236. TOKYO, Japan, May 2019.
4. **Hossain E**, Habiba U, Matsuda AY, Kitamura T, Higashino F, Application study of newly developed adenovirus.
   The 4th Hokkaido University cross-department symposium. P-59.Sapporo, Japan, January 2019.

# Chapter I

# General Introduction

## 1. Introduction

Almost 70% of death are caused by noncommunicable diseases (NCDs) in the world. This includes heart disease, stroke, cancer, diabetes, and chronic lung diseases (WHO 2020). Cancer is the uncontrolled cell growth with the potential to invade or spread to other parts of the body. Agents that may cause a normal body cell to develop abnormality can cause cancer; there are many causative agents such as chemical or toxic compound exposures, radiation, pathogens, and genetic mutations ( Anand et al., 2008*;* Davis et al., 2020). There are some common environmental elements that contribute to cancer including tobacco (25–30%), food habit and obesity (30–35%), infectious disease (15–20%), radiation (both ionizing and non-ionizing, up to 10%), sedentary lifestyle, and pollution (Anand et al., 2008; Islami et al.,2018; Cohen et al., 2019). The most common type of cancers is; breast cancer, skin cancer, lung cancer, colon cancer, prostate cancer, lymphoma, carcinoma, sarcoma, melanoma, and leukemia.

To date, cancer is the second-leading cause of globally (WHO 2018), excluding any kind of endemic diseases like COVID-19. Despite the advancement in treatment options for cancer, it remains the leading cause of mortality and morbidity worldwide. Hopefully, the survival rates are improving for many types of cancer, thanks to improvements in cancer screening and cancer treatment. Besides the conventional treatment approaches like chemotherapy or radiotherapy, new modalities have emerged, such as immunotherapy and oncolytic virotherapy.

### 1.2 The conventional method of cancer treatment

There are many methods for treating cancer, depending on the type of cancer, grading, staging, types of treatment are available, and the goals of treatment. The cancer treatment categories include a range of procedures, machines, drugs, and/or approaches. The most commonly available treatment options are; surgery, chemotherapy, radiotherapy, targeted therapy and gene therapy.

The treatment option may be the combination of two existing modalities to target as many cancer cells as possible. The goal is to achieve the highest level of potential efficacy with the lowest level side effect.

## 1.3 Gene Therapy

Gene therapy holds unique promise by offering a means of specific targeting of tumor genes that promote malignant behavior and treatment resistance (Wang et al., 2016). Usually, cancer develops by abnormal growth factor signaling, which initiates a cell to grow and divide develops constitutively active. These are occurred by oncogenes via mutations in proto-oncogenes such as a growth factor receptor and resulted in the abnormal cell signaling pathways. Hence, to successfully treat cancer, the oncogene must be destroyed; otherwise, cancer will continue to grow and spread (Gene Therapy Review 2020).

To date, successful trials of gene therapies have been reported in patients with chronic lymphocytic leukemia, acute lymphocytic leukemia, brain tumors, and others. However, only a few gene therapy products are available for clinical use such as ONYX-015 and Gendicine for refractory head and neck cancer. (Wang et al., 2016). There are various types of gene therapy, recognized by ongoing clinical trials worldwide. The aim of these strategies is to destroy cancer cells without harmful effects on normal cells. This can be achieved by the following approaches.

**Gene therapy approaches:**

1. Oncolytic virotherapy
2. Expression of the tumor suppressor gene
3. Immunotherapy
4. Gene-directed enzyme prodrug therapy
5. Expression of genes that initiate cell death

## 1.4 Oncolytic virotherapy

Oncolytic virotherapy is a promising anti-cancer therapy. From the past few decades, it has been known that some viruses can kill cancer cells if they are able to replicate inside them. Currently, oncolytic viruses (OVs) are using an anti-cancer drug (Table-1). OVs therapy was first demonstrated in the 1990s when a recombinant thymidine kinase (TK)-negative herpes simplex virus (HSV-1) showed tumor cell killing capacity (Fu et al., 2019). OVs infect and kill cancer cells with little to no effect on healthy tissue (Hao et al., 2019; Jenner et al., 2018). To date, research is being

conducted around the world using both non-engineered and engineered OVs to explore their efficacy against multiple types of cancer. Natural OVs or with genomic editing can target and replicate certain types of tumor cells. However, these unedited viruses are not tumor-specific, or they can harm normal cells as well (Figure 1.1), such as Reovirus, Senecavirus, Vaccinia virus, and adenovirus (Fu et al., 2019).

**Table 1: Oncolytic viruses used as an anti-cancer drug**

| Name | Targeted Tumor | Type of virus | Country |
|---|---|---|---|
| **Oncorine** | Head and neck | Adenovirus type 5 | China (2005) |
| **T-VEC** | Malignant Melanoma | Herpes simplex virus | USA (2015) |

Source: www.sunwaybio.com, www.imlygic.com

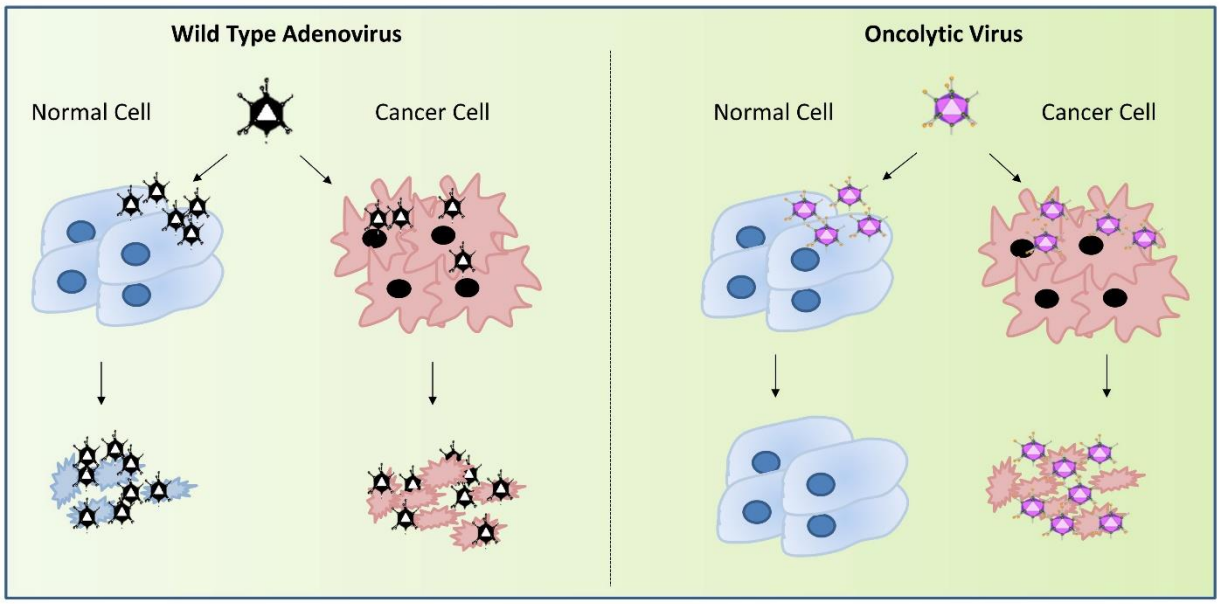


Figure 1.1. Cancer-selective replication of the oncolytic virus

On the other hand, the engineered virus can selectively target and/or replicate in specific cancer cells. Such as adenovirus, reovirus, measles, herpes simplex, newcastle disease virus, and vaccinia have been clinically tested as oncolytic agents (Donnelly et al., 2012). Most current oncolytic viruses are engineered for tumor selectivity. There are many ways to develop OVs, either modifying viral genes by mutation or by the

insertion of cancer-specific agents (Abul El Hassan et al., 2004). The current status of oncolytic virotherapy in Japan is discussed in Table 2.

**Table 2: Current status of oncolytic virotherapy in Japan.**

| Precursor virus | Virus | Phase | Tumor | Institute | Status |
|---|---|---|---|---|---|
| **HSV-1** | T-VEC (talimogene laherparepvec; IMLYGIC®; OncoVEXGM-CSF | I | Unresectable Stage IIIB–IV malignant melanoma | Multicenter | Underway |
| **HSV-1** | G47Δ | I–IIa | Glioblastoma | The University of Tokyo | Completed |
| **HSV-1** | | II | Glioblastoma | The University of Tokyo | Underway |
| | | I | Castration-resistant prostate cancer | The University of Tokyo | Completed |
| | | I/IIa | Olfactory neuroblastoma | The University of Tokyo | Underway |
| | | I/IIa | Malignant mesothelioma | The University of Tokyo | Planned |
| **HSV-1** | HF10 (Canerpaturev; C-REV) | I | Metastatic breast cancer | Nagoya University | Completed |
| | | I | Recurrent head and neck cancer | Nagoya University | Completed |
| | | I | Pancreatic cancer | Nagoya University | Completed |
| | | I | Malignant solid tumors | Mie University | Terminated |
| | | I | Advanced unresectable pancreatic cancer | Nagoya University | Completed |
| | | I | Solid tumors with superficial lesions | National Cancer Center Hospital | Completed |
| | | II | Unresectable or metastatic melanoma | Multicenter | Underway |
| | | I | unresectable pancreatic cancer | Multicenter | Planned |

| | | | | | |
|---|---|---|---|---|---|
| **Adenoviruses** | Telomelysin (OBP-301) | I/II | Esophageal cancer | Okayama University | Underway |
| | | I | Esophageal cancer | Unpublicized | Planned |
| | | I | Advanced solid tumors | National Cancer Center Hospital East | Planned |
| | Surv.m-CRA | I | Advanced solid tumors | Kagoshima University | Underway |
| **Sendai virus (HVJ)** | Sendai virus particle (HVJ-E; GEN0101; TSD-0014) | I/II | Castration-resistant prostate cancer | Osaka University | Completed |
| | | I | Castration-resistant prostate cancer | Osaka University | Underway |
| | | I/II | Malignant melanoma | Osaka University | Underway |
| | | I | Malignant melanoma | Osaka University | Underway |

*(Taguchi 2018)*

### 1.5 Oncolytic Adenovirus

Among all the oncolytic viruses, using adenoviruses (Ads) is much more attractive because of their high proliferation ability *in vitro*. Ads were first isolated in 1953 from human adenoid cells (Rowe et al.,1953). The Ads are non-enveloped viruses with double-stranded linear DNA about 35kbp length. Human Ads are classified into seven subgroups (A–G). Among them, serotype 5 (Ad5), which belongs to subgroup C, is more extensively used in gene therapy and virotherapy (Rux & Burnett, 2004). The viral genome consists of early (E) and late (L) genes (Berk et al., 2006). The early genes include E1, E2, E3, and E4 and they regulate viral replication through modification of host cells (Russel et al., 2000). The early gene 1A, a subunit of the E1 gene, is the first expressed gene after infection of modulating the cell cycle of host cells and regulate the expression of cellular and viral genes (Abudoureyimu et al., 2019). E1B gene usually codes two proteins called E1B-55k and -19kDa. The primary function of E1B is to prevent apoptosis in adenovirus infected cells. E1B-55k blocks p53 and halt its action from inducing apoptosis ( Debbas et al., 1993). The late genes encode structural proteins L1,

L2, L3, L4, and L5. These proteins package the viral DNA into the virion in the final stages of replication.

The adenovirus life cycle is separated by the DNA replication process into two phases: an early and a late phase. The early phase occurs inside the nucleus and produces early genes. These early genes products produce early viral mRNA via transcription and transfer to the cytoplasm of the host cell. After further translation of mRNA produces early viral proteins. E2F protein force the host cell into S-phase of the cell cycle. The late phase produces the late genes which undergo transcription to produce late viral mRNA and after the final translation of mRNA form the late viral structural protein.

After completion of mRNA translation, all the virion proteins get assembled and viral DNA packaged into the capsid, and this process is called maturation. Finally, the progeny virus released by cell lysis or budding to infect the adjacent cells.

There are three main tactics to develop tumor-selective oncolytic adenoviruses as follows.

**1.Targeting Capsid Modification**

The capsid is the external surface of the virus and is composed of hexon, penton, and projectile fibers (Knipe and Howly, 2001). These capsid proteins can be modified so that the virus will only target cancer cells. Caspid modified virus upregulates the attachment with the primary receptor and also, they showed potent anti-cancer effects by IV injection.

**2. Selective Replication by deletion of an Antitumor Gene**

Oncolytic adenovirus can be engineered by the deletion of certain genes, which are vital to viral replication in normal cells but dispensable in tumor cells. Such as “E1B-55k deleted” H101 virus (Bischoff et al., 1996). H101 virus can replicate only in the absence of the p53 gene; thus, it fails to replicate in normal cells.

**3. Selective Replication by Insertion or Arming of Certain Gene, cytokines, Drugs or Antigen**

Adenovirus can be modified by inserting genes, such as a transcriptional promoter only activated in cancer cells or arming with certain drugs or receptor genes. These viruses are modified so that they will replicate only in the presence of certain characteristics. They normally triggered replication in cancer cells and leading to cancer cell death (Gene Therapy Review, 2020).

## 1.6 Engineering oncolytic adenovirus by inserting ARE in the 3'-untranslated region

We developed an adenovirus designated Ad-*fos*ARE by inserting AU-rich element (ARE) of *c-fos* gene in the 3'-untranslated regions (3'-UTR) of the E1A gene (Figure 1.2).

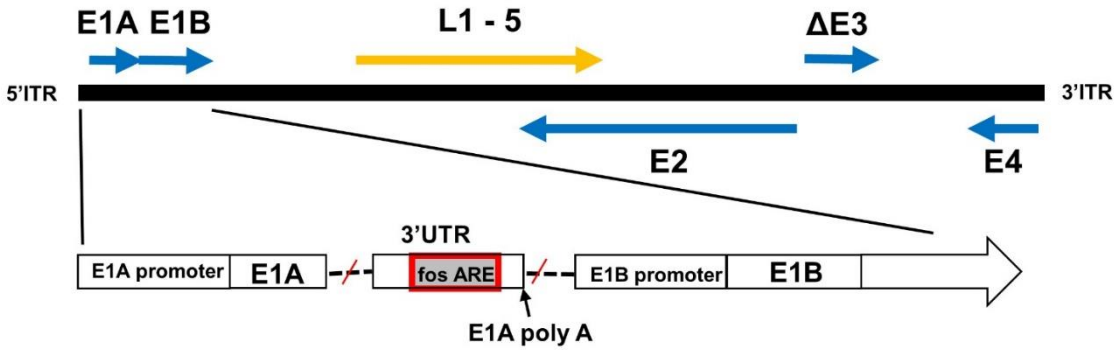


Figure 1.2. Structure of Ad-*fos*ARE virus

### 1.6.1 Construction of Ad-*fos*ARE

Ad-*fos*ARE was constructed using a pXhoIC plasmid and pAdenoX-PRLS (Clontech). pXhoIC has the E1 region of the type 5 human adenovirus genome. A 69-base pair of synthesized ARE fragment (5'- ttttattgtg tttttaattt atttattaag atggattctc agatatttat atttttattt tatttttt -3') of the *c-fos* gene was inserted into the HpaI site in the 3'-

UTR of the E1A gene in pXhoIC. A fragment of the E1 region was then amplified by PCR, and inserted into the deleted E1 region of the adenovirus genome in the pAdenoX-PRLS by in-fusion technique (Fw: 5' gtaactataacggtcatttgtctagggccgcggggactt-3', Rv: 5'-attacctctttctccgccacgcccacacatttcagtacc-3'). The entire genome of Ad-*fos*ARE was isolated by cutting using PacI and the fragment was then transfected into 293 cells. Virus particles were concentrated by several rounds of viral infection and cells were collected in order to prepare a virus lysate by subjecting them to three cycles of freezing and thawing. The titers of the infectious unit (ifu) of Ad-*fos*ARE were determined using the Adeno-XTM Rapid Titer Kit (Clontech) and 293 cells according to the manufacturer's instructions.

### 1.6.2 What makes Ad-*fos*ARE is cancer-selective?

**AREs**

AREs are the targets for rapid degradation of mRNA and the fate of ARE-mRNA is controlled by several RNA-binding proteins, such as HuR. In cancer cells, there is an abundance of cytoplasmic HuR exportation, so mRNA can stabilize.

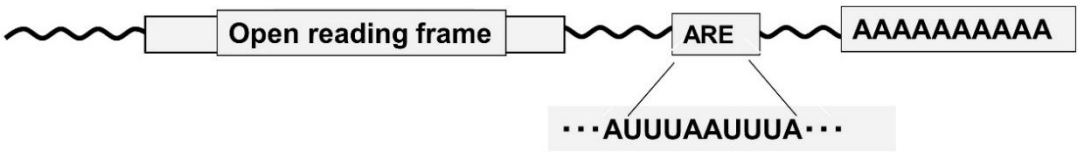


Figure 1.3. Adenosine- and uridine-rich elements (AREs)

AREs are usually located in the 3'-UTR of mRNAs and are the best-known determinants of mRNA instability (Figure 1.3). Studies on the expression of cytokines and proto-oncogenes have shown that many 3'-UTRs contained AREs and subsequently, some of their translation are controlled by these AREs (Espel et al., 2005, Kruys et al., 1987,1989). AREs are primarily defined by their ability to promote rapid de-adenylation-dependent mRNA decay (Kruys et al., 1989). There is relatively lesser sequence similarity among AREs, the *c-fos* mRNA with the most typical ARE contains

AUUUA pentamers and/or U-rich sequences (Espel et al., 2005; Chen et al., 1995). AREs control mRNA degradation and translation via interactions with RNA binding proteins, which specifically bind to ARE. mRNAs carrying AREs are considered unstable and are translated only for a short period, as in the case for transcription factors, cytokines, oncogenes, and certain RNA transcripts of DNA viruses (Chen et al., 1995; Nadar et al., 2011).

Cellular RNA binding proteins, such as Tristetraprolin (TTP), ARE/poly (U)-binding/degradation factor 1 (AUF 1), Hu antigen R (HuR), and T-cell internal antigen-1 (TIA-1), bind to mRNAs that contain AREs. ARE binding proteins (AREBPs) either aim for the mRNA to enter the degradation pathway, (TTP and AUF1) (Nadar et al., 2011, DeMaria et al., 1996), or protect the mRNA from degradation (HuR), or suppress their translation (HuR and TIA) (Yeh et al., 2008) (Figure 1.4).

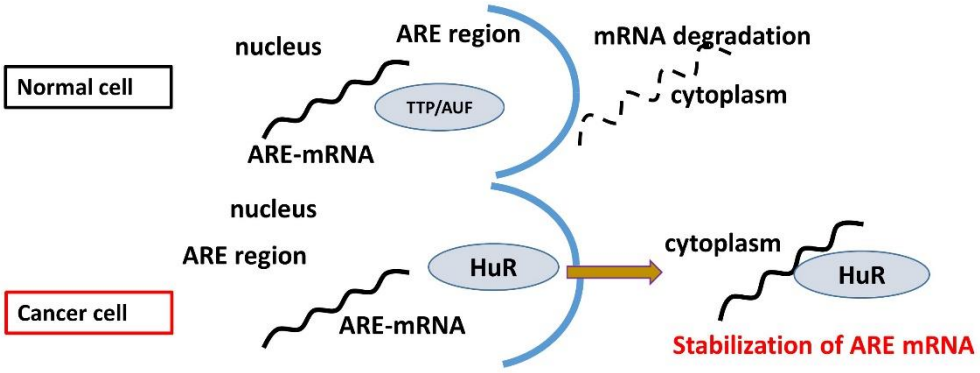


Figure 1.4. Degradation and Stabilization of ARE mRNA.

**HuR and stabilization of mRNA**

HuR is a member of the embryonic lethal abnormal vision (ELAV) family of RNA-binding proteins, which is ubiquitously expressed by the most type of cells. Intracellularly, HuR is localized mainly in the nucleus but shuttles between the nucleus and the cytoplasm (Habiba et al., 2016, Fan et al.,1998). Cytoplasmic HuR protects ARE-mRNAs against rapid degradation by binding with ARE (Brennan et al., 2001). In normal cells, HuR transiently relocalizes to the cytoplasm under stress conditions. In contrast, in cancer cells, HuR is constitutively localized in the cytoplasm and speculated to be involved in the ARE-mRNAs stabilization and transformation of cancer cells (Silanes et al., 2003,2005, Kuroshima et al., 2011).

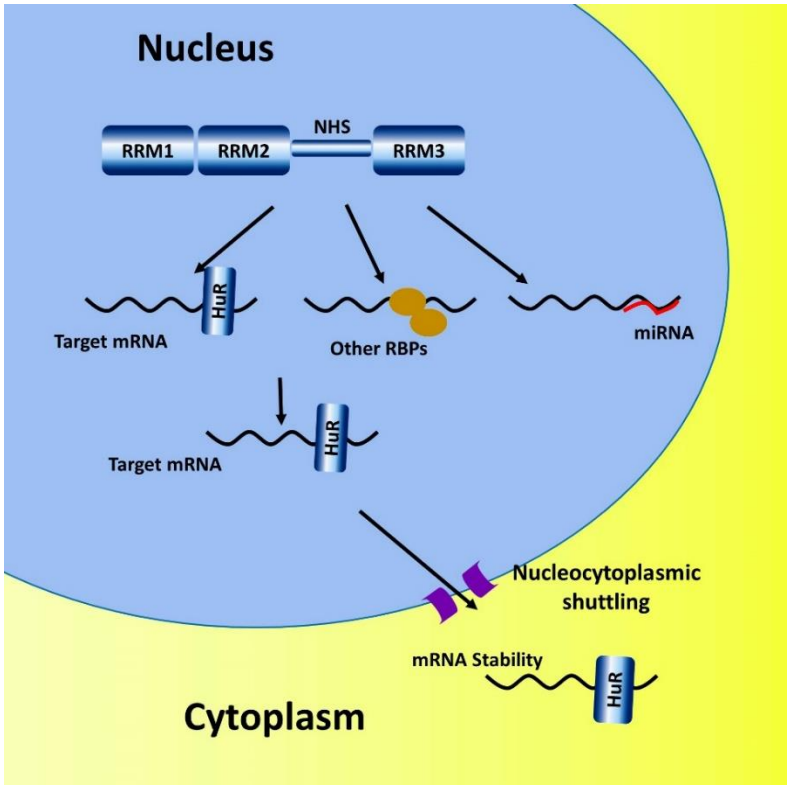


Figure 1.5. HuR and stabilization of ARE-mRNA

## 1.7 Hypothesis

For Ad-*fos*ARE replication, cytoplasmic HuR relocalization and ARE-mRNA stabilization are necessary. In normal cells, where there is no cytoplasmic HuR, E1A mRNA is degraded soon after its synthesis due to the existence of ARE. On the other hand, it is stabilized in cancer cells, resulting in the replication of Ad-*fos*ARE and lyse cancer cells. This is the theory that makes Ad-*fos*ARE cancer-selective.

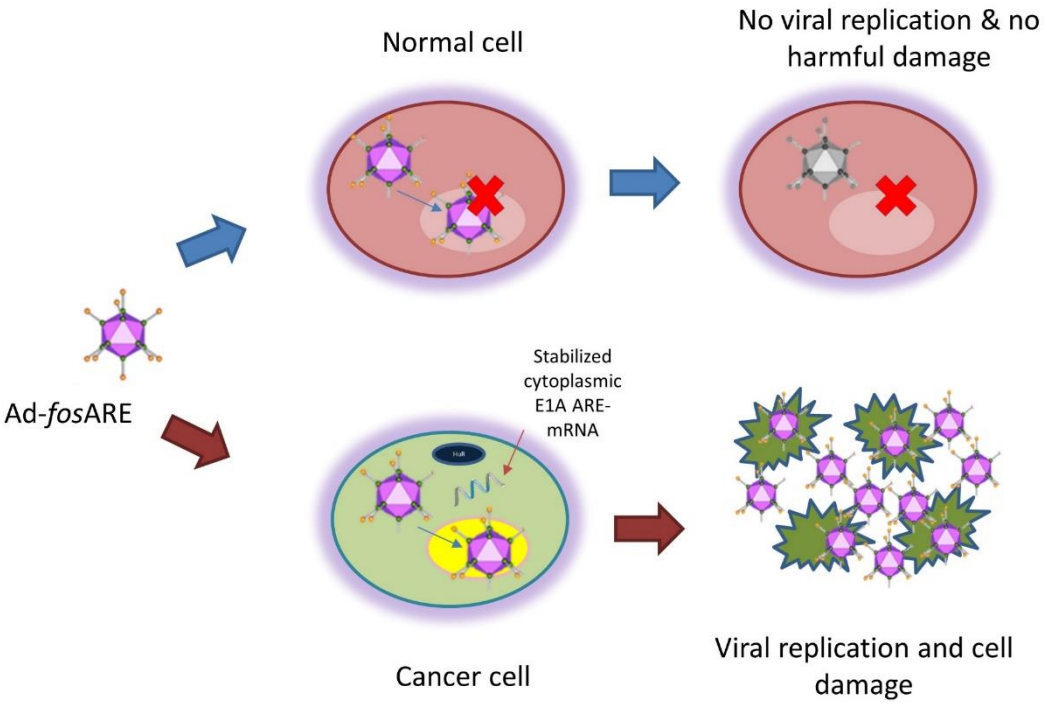


Figure 1.6. Cancer-selective replication of Ad-*fos*ARE

## 1.8 Objectives:

### General objective

To develop a potential conditionally replicative adenovirus (CRADs) by inserting *c-fos* ARE in the 3' UTRs of the E1A gene.

### Specific Objective:

1. To investigate the cancer-selective replication and cytolytic activity of Ad-*fos*ARE.

2. To evaluate the dependency on stabilized ARE-mRNA for Ad-*fos*ARE replication by manipulating HuR.

3. To compare the efficacy of Ad-*fos*ARE with dl1520 and WT300 in terms of less normal cell damage.

4. To investigate the synergistic effect of the combination treatment with chemotherapy.

5. To assess the increased mRNA stabilization by chemotherapy.

6. To find out the effect of the upregulated coxsackie-adenovirus receptor (CAR) expression and stabilized microtubules on viral uptake and release.

7. To investigate *in vivo* cytolytic activity of Ad-*fos*ARE and synergistic effect of combination treatment.

**Table-3: List of Acronyms**

| List of Acronym | |
|---|---|
| **Ad** | Adenovirus |
| **Ad5** | Adenovirus serotype S |
| **ARE** | Adenylate-uridylate-rich element |
| **AUF-1** | ARE/poly (U)-binding/degradation factor |
| **CAR** | Coxsackie-adenovirus receptor |
| **CPE** | Cytopathic effect |
| **CRADs** | Conditionally replicative adenovirus |
| **DNA** | Deoxyribonucleic acid |
| **ELAV** | Embryonic lethal abnormal vision |
| **GAPDH** | Glyceraldehyde 3 phosphate dehydrogenase |
| **HuR** | Human Antigen R |
| **HS** | Heat shock |
| **HSV** | Herpes simplex virus |
| **ifu** | Infectious unit |
| **i.t.** | Intra-tumoral |
| **i.p.** | Intraperitoneal |
| **i.v** | Intra-venus |
| **IMRT** | Intensity-modulated radiotherapy |
| **KD** | Knockdown |
| **MOI** | Multiplicity of infection |
| **OV** | Oncolytic Virus |
| **PARP** | Poly(ADP-ribose )polymerase |
| **PBS** | Phosphate buffered saline |
| **PCR** | Polymerase chain reaction |
| **PTX** | Paclitaxel |
| **mRNA** | Messenger RNA |
| **MTs** | Microtubules |
| **NCDs** | Noncommunicable diseases |

| | |
|---|---|
| **RBP** | RNA binding protein |
| **RNA** | Ribonucleic acid |
| **RT-PCR** | Real-time polymerase chain reaction |
| **SDS** | Sodium Dodecyl Sulphate |
| **SDS-P AGE** | SDS polyacrylamide gel electrophoresis |
| **siRNA** | small interfering RNA |
| **TIA-1** | T-cell internal antigen-1 |
| **TK** | Thymidine kinase |
| **TTP** | Tristetraprolin |
| **vp** | viral particle |
| **UTRs** | Untranslated region |
| **WT** | Wild type |

## Chapter II

# Oncolytic Potential of Conditionally Replicative Adenovirus Controlled by the Stabilization System of AU-rich Elements-Containing mRNA

## 2.1. Introduction

Viral therapy based on conditionally replicating adenoviruses (CRAds) is a promising cancer therapeutic strategy, as these viruses selectively replicate and lyse cancer cells (Alemany et al., 2000, Kim et al., 2000). CRAds are obtained by, either modifying viral gene by mutation, and by insertion of cancer-specific agents (Abou El Hassan et al., 2004). We developed an adenovirus designated Ad-*fos*ARE by inserting *c-fos* AU-rich elements (ARE) in the 3'-untranslated region (3'-UTR) of the E1A gene.

In this study, we investigated the potential of adenovirus Ad-*fos*ARE as oncolytic virus. The replication of this virus was markedly high in cancer cells compared with that in normal cells. The propagation and cytolytic activity of this virus in cancer cells were similar to dl1520 (equivalent to H101), which is clinically applied (Bischoff et al., 1996, Kasuya et al., 2005). But in normal cells viral replication and cytotoxicity of Ad-*fos*ARE were less than E1B55k-deleted adenovirus. These findings indicate that Ad-*fos*ARE is a potential oncolytic virus.

## 2.2. Material and Method:

### 2.2.1 Cell lines:

Cell lines used in this study are described in Table-2.1. Cells were acquired from the American Type Culture Collection (ATCC; Manassas, VA, USA) and cultured in Dulbecco's modified Eagle's medium (DMEM; Sigma-Aldrich; Merck KGaA, Darmstadt, Germany) including 10% fetal bovine serum (FBS; Biowest, Nuaille, France) with antibiotics at 37 °C in a 5% $CO_2$ atmosphere in humidified conditions.

**Table 2.1: Cell lines**

| Cell line | Description | Features | Condition of p53 |
|---|---|---|---|
| **A549** | Human lung adenocarcinoma cells | | Wild type |
| **H1299** | Human non-small lung carcinoma cell line | | null |
| **HeLa** | Human Cervical cancer cell | HPV-18 + | Wild type |
| **HeLa S3** | a clonal derivative of the parent HeLa line | HPV-18 + | deficient in *p53* |
| **C33A** | Human Cervical cancer cell | HPV - | Mutant p53 |
| **U2OS** | Human Bone Osteosarcoma Epithelial Cells | | Wild type |
| **HepG2** | Human liver cancer cell line | no hepatitis B virus surface antigens | Wild type |
| **293** | Transformed human embryonic kidney cells | Express E1A region | Wild type |
| **BJ** | Human fibroblast skin | | Functional p53 |
| **HGF1** | Human gingival fibroblast | | Functional Wild type |

### 2.2.2.Adenoviruses:

Newly constructed Ad-*fos*ARE, Wild-type adenovirus type 5 (WT300) (generous gift from Dr T. Shenk; Princeton University), E1B55k-deleted mutant adenovirus (dl1520) (generous gift from Dr A.J. Berk; University of California) were used in this study.

### 2.2.3.Drug, reagents, and antibodies

Actinomycin D (from Streptomyces species) were purchased from Sigma-Aldrich (USA). Antibodies used in this study are described in Table-2.2

**Table 2.2: Antibodies used in this study.**

| 1st antibodies | 2nd antibodies | Molecular weight | Dilutions | Source |
|---|---|---|---|---|
| **E1A** | Mouse | 30~50 kDa | 1:1000 | Santa Cruz Biotechnology |
| **E1B** | Mouse | 55 kDa | 1:10 | Gift from T Shenk |
| **L133** | Rabbit | 110,70,60 kDa | 1:5000 | Gift from T Dobner |
| **CAR** | Mouse | 46 kDa | 1:200 | Santa Cruz Biotechnology |
| **HuR** | Mouse | 36 kDa | 1:5000 | Santa Cruz Biotechnology |
| **ACTIN HRP** | - | 43 kDa | 1:5000 | Santa Cruz Biotechnology |
| **β-TUBULIN** | Mouse | 52 kDa | 1:5000 | Millipore Corp |
| **LAMIN B** | Goat | | 1:5000 | Santa Cruz Biotechnology |
| **PARP** | Rabbit | 46kDa | 1:1000 | Cell Signaling Technology |
| **Acetylated tubulin** | Mouse | 52kDa | 1:1000 | Millipore Corp |
| **Detyrosinated tubulin** | Rabbit | 52kDa | 1:1000 | Millipore Corp |

### 2.2.5. Preparation of Ad-*fos*ARE, WT300 and dl1520 virus stock

To prepare virus stock, Ad-*fos*ARE, WT300 and dl1520-infected 293 cells were harvested by centrifugation to avoid aspirate non-adherent cells, and then they were subjected to three cycles of freezing and thawing. Viral titers infectious units (ifu/ml) were counted using the Adeno-X™ Rapid Titer kit (Clontech Laboratories, Inc., Mountain View, CA, USA) according to the manufacturer's directions. Virus particles (vp/ml) were determined by a QuickTiter Adenovirus Quantitation kit (Cell Biolabs, San Diego, CA, USA).

### 2.2.6. Western blot analysis

Cells were lysed with RIPA buffer (150 mM NaCl; 25 mM Tris-HCl, pH 7.6; 1%Nonidet P-40; 1% sodium deoxycholate; 0.1% SDS) containing protease inhibitors. An equal amount (20 μg) of total protein were separated by 10% sodium dodecyl sulfate-polyacrylamide gel electrophoresis (SDS-PAGE) and transferred onto polyvinylidene difluoride membranes (Millipore, Billerica, MA, USA). Fractionation buffer (10 mM Tris-HCl, pH 7.6, 150 mM NaCl, 1.5 mM $MgCl_2$, 0.5% Nonidet P-40, protease inhibitor cocktail) was used to separate the cells into the cytoplasmic and nuclear fractions, followed by vigorous shaking for 5 min and centrifugation at 12,000 rpm for 30 s. The supernatant was used as the cytoplasmic protein fraction. To assess the accuracy of cell fractionation, cytoplasmic (β-tubulin) and nuclear (lamin B) proteins were detected. Bands were visualized using SuperSignal West Femto Maximum Sensitivity Substrate (Thermo Fisher Scientific, Inc., Waltham, MA, USA).

### 2.2.7.*In vitro* virus proliferation assay

Cancer cells and normal cells were seeded into 12-well plates at a density of $5\times10^4$ cells/well 24 h before the infection. Cells were infected with Ad-*fos*ARE, dl1520, or WT300 at an MOI of 10 ifu/cell and the medium was not changed after virus infection. After incubation at 37 °C for 72 h, cells were collected, and a virus lysate was prepared as described above. Viral titers (ifu/ml) were determined using the Adeno-X Rapid Titer kit (Clontech Laboratories).

### 2.2.8. HuR depletion

For HuR knockdown, Lipofectamine RNAiMAX (Invitrogen; Thermo Fisher Scientific) was used to transfect HeLa cells with 20 nM each siRNA targeting HuR 1 (5'-AAG UGC AAA GGG UUU GGC UUU UU-3') or HuR 2 (5'-AAU CUU AAG UUU CGU AAG UUA UU-3') or HuR 3 (5'-UUC GUA AGU UAU UUC CUU UAA UU-3') with a negative control siRNA (5'-TCT TAA TCG CGT ATA AGG CTT-3'; Qiagen, Hilden, Germany). After 48 h of transfection, HeLa cells were infected with Ad-*fos*ARE. After 48 h of infection, all cells were scrapped off, and the virus lysate was prepared by three freeze-thaw cycles. Viral titers were detected by using the Adeno-X Rapid Titer kit (Clontech Laboratories) and 293 cells.

For heat shock treatment, HeLa cells were kept at 43 °C for 2 h and immediately infected with Ad-*fos*ARE. And after 24 h the infected cells were heat-shocked (2 h) again. Cells were incubated at 48 h after infection, and the viral titers were determined as described above.

### 2.2.9. RNA extraction and quantitative RT-PCR

Total RNA was extracted using the RNeasy Mini Kit (250) from QIAGEN and the RNA was subjected to reverse transcription by ReverTra Ace qPCR RT master mix with genomic DNA remover (Toyobo, Osaka, Japan). Quantitative RT-PCR was performed in the DNA Engine Opticon2 (MJ Research, Watertown, MA, USA), and cDNA was amplified using the following primers: Ad5 E1A; 5'-gaa cca ccta ccc ttc acg-3', 5'-ccg cca aca tta cag agt cg-3', GAPDH; 5'-atc ctg ggc tac act gag ca-3', 5'-tgc tgt agc caa att cgt tg-3'. GAPDH was used for normalization. To evaluate the E1A mRNA, HeLa cells were heat-shocked and cellular RNA of each cell was used for quantitative RT-PCR. To estimate the half-life of total E1AmRNA, cells were treated with 5μl/mL Actinomycin D 60, 120, or 180 min. The total cellular RNA of each cell was used for quantitative RT-PCR.

### 2.2.10. Cytopathic effect (CPE) assay and cell viability assay

Cancer and normal cells were seeded on 24-well plates ($5\times10^4$ cells/well). 24 h later, the cells were infected with Ad-*fos*ARE at a multiplicity of infection (MOI) of 1, 10,50, and 100 ifu/cell and maintained for an additional 7 days. Then cells were fixed and stained with Coomassie brilliant blue.

A 2-3-bis [2-methoxy-4-nitro-5-sulfophenyl]-2H-tetrazolium-5-carboxanilide inner

salt assay was used to observe the cytolytic activity. Cells were seeded on 96-well plates at 3×103 cells/well. 24 h later, the cells were infected with Ad-*fos*ARE at an MOI of 100 ifu/cell. Cytolytic activity was assessed using an XTT assay on days 1, 3, 5, and 7 with the Cell Proliferation kit II (Roche Diagnostics, Basel, Switzerland) according to the manufacturer's protocol.

### 2.2.11. Immunocytochemistry

Cells were grown on coverslips in 35-mm dishes at 60–80% confluence and treated with virus and drug for Hoechst 33342 staining for detection of cell death. After treatment, cells were rinsed once with phosphate buffer saline (PBS), fixed for 20 min at RT with 4% paraformaldehyde in PBS, blocked and permeabilized in 2% BSA plus 0.1% Triton X-100 in PBS at room temperature. Cell nuclei were stained with Hoechst 33342 before mounted on slides by using Mountant permafluor (Thermo scientific, FM 111212A). Cells were observed using an IX71 inverted microscope (Olympus). Image acquisition was performed with the Olympus FluoView Software (FV10-ASW Viewer, ver.4.2).

## 2.3 Results

### 2.3.1. Cancer-Selective replication of Ad-*fos*ARE

The Adenoviral genome consists of four early genes (E1–E4) and five late genes (L1–L5). Early genes are responsible for virus replication, and late genes code capsid proteins. After viral infection, the E1 gene is expressed first and then controls the expression of other viral genes (Abudoureyimu et al., 2019). To examine the expression of E1A (30~50 kDa) protein, two kinds of cancer cells (HeLa, A549) and normal cells (BJ) were infected with Ad-*fos*ARE at an MOI of 100 (ifu/cell) for 96 h (Figure 2.1). E1A expression was found 72 h after infection in cancer cell HeLa and A549 (Supplementary Figure 1). But in BJ cells, we could not get clear E1A expression. A similar result was found for E1B-55k. In this study, we used WT300 as a positive control because it shows viral protein expression both in cancer and normal cells and non-treated cells as a negative control. We also assessed Actin as a loading control.

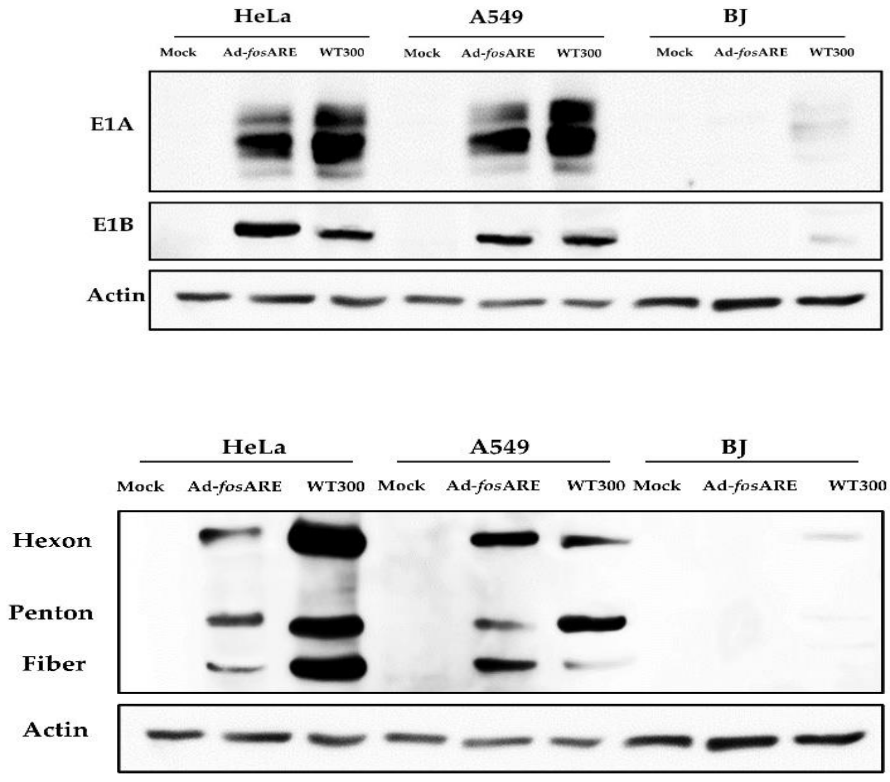

**Figure 2.1.** Expression of early and late virus protein in Ad-*fos*ARE and WT300-infected cells. (A) HeLa, A549 and BJ cells were infected by both viruses for 96 h and the expression of early proteins E1A and E1B were examined. (B) Late protein hexon, penton, and fiber were estimated by western blot analysis. Actin expressions were also assessed as the internal control.

We also examined the expression of late viral protein hexon, penton and fiber (Figure 2. 1). Cells were treated with Ad-*fos*ARE 96 h and the whole lysate was collected and subjected to western blot analysis. The results were similar to E1A expression. In cancer cells, we found both E1B-55k and late gene products but not in normal BJ cells.

To examine the production efficiency of Ad-*fos*ARE, cancer cells (HeLa, C33A, A549 and H1299) and normal cells (BJ) were infected with at an MOI of 10 ifu/cell and virus titers generated after 48 h and detected by staining the hexon protein of virus particles. In cancer cells, the propagation of Ad-*fos*ARE was very high. On the other hand, the titer in normal cells was 3 to 4 logs lower than those in cancer cells (Figure 2.2). These results indicate that Ad-*fos*ARE can selectively replicate in cancer cells.

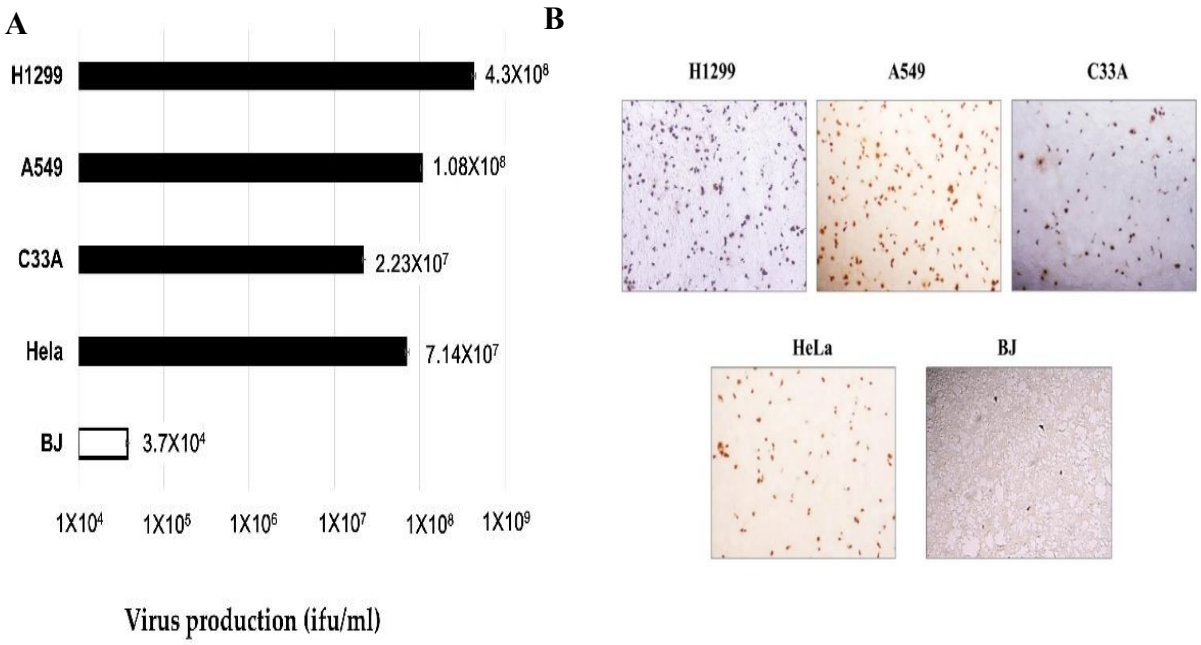

**Figure 2.2**. The production efficiency of Ad-*fos*ARE. Cancer (HeLa, C33A, A549 and H1299) cells and normal (BJ) cells were infected with Ad-*fos*ARE at an MOI of 10 ifu/cell and virus production was determined 48 h after infection. (A) Each titer (ifu/ml) is shown on the graph. Data are shown above as the mean ± standard deviation of three independent experiments. (B) The hexon staining in 293 cells used to count virus titers.

### 2.3.2. HuR-mediated mRNA stabilization is essential for adenovirus replication

In order to investigate whether Ad-*fos*ARE replicates in an ARE-mRNA stabilization-dependent manner, Ad-*fos*ARE replication was examined using conditions that decrease ARE-mRNA stabilization and conditions that enhance stabilization conversely. To evaluate virus production in HuR-depleted cells, where ARE-mRNA cannot be stabilized, we treated cells with heat shock (HS), as a previous survey revealed that heat shock transiently decreases HuR abundance (Abdelmohsen et al., 2009). HS treatment of HeLa cells for 2 h resulted in reduced expression of HuR protein in the cytoplasm of cells and also shortened the half-life of E1A mRNA containing ARE (Figure 2.3.C bottom). Likewise, HS-treated cells showed a significant reduction in virus production compared to the non-treated cells (Figure 2.3.B).

**A**

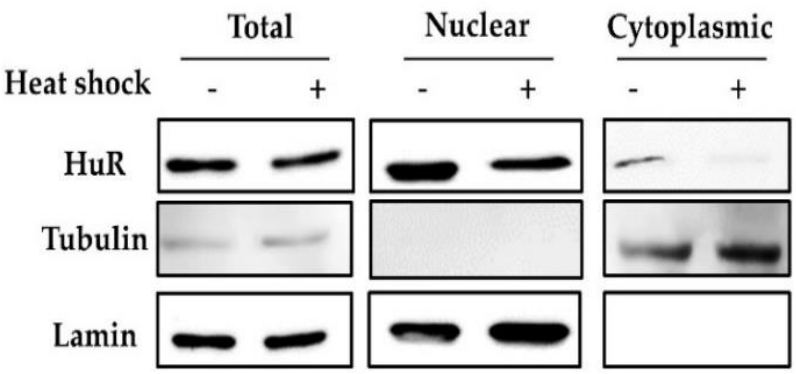
Total
Nuclear
Cytoplasmic
Heat shock
- + - + - +
HuR
Tubulin
Lamin

**B**

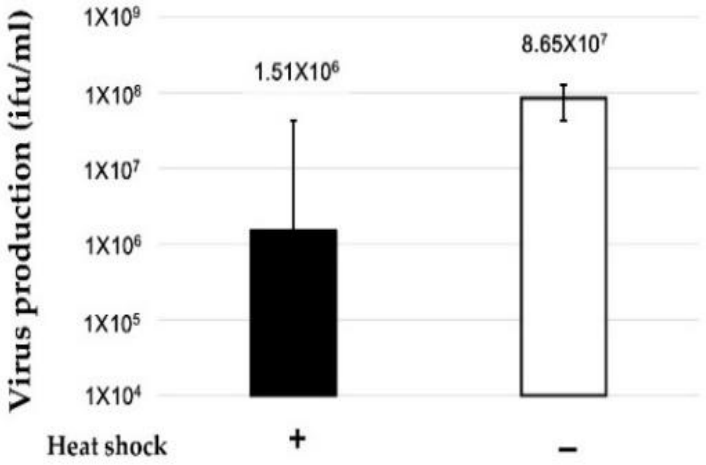
Virus production (ifu/ml)
1X10⁹
1X10⁸
1X10⁷
1X10⁶
1X10⁵
1X10⁴
1.51X10⁶
8.65X10⁷
Heat shock
+
–

**C**

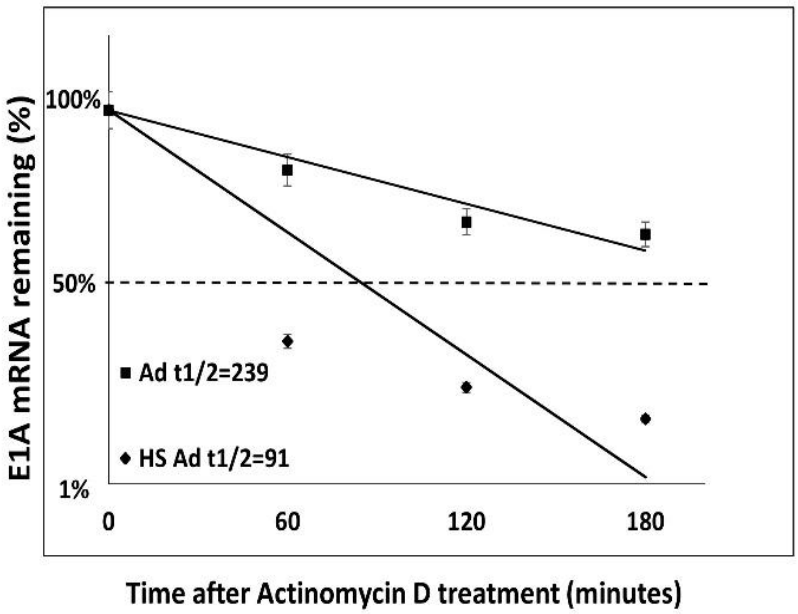
E1A mRNA remaining (%)
100%
50%
1%
Ad t1/2=239
HS Ad t1/2=91
0
60
120
180
Time after Actinomycin D treatment (minutes)

**Figure 2.3.** The effects of HuR-depletion on E1A mRNA stabilization and Ad-fosARE replication. (A) HeLa cells were heat-shocked at 43˚C for 2 h and the amount of HuR in the total, the nuclear and cytoplasmic fraction was determined using western blot analysis. β-tubulin and lamin expression were also identified as the markers of the cytoplasm and nuclear fractions. (B) Virus production was then assessed, and the values were compared to the non-treated cells (middle). (C) HeLa cells were infected with Ad-*fos*ARE (MOI 10 ifu/cell) and heat-shocked immediately after infection at 43˚ C for 2 h. Transcriptions were inhibited by actinomycin D 5μg/mL for 60, 120 and 180 minutes. After the indicated periods, cells were harvested and extracted for total cellular RNA. mRNA levels are quantified by quantitative RT-PCR experiments using GAPDH as a normalization control. Graphs depict the percentage of remaining E1A mRNA levels with GAPDH mRNA and compared with the standards of normalized mRNA species measured immediately after the addition of actinomycin D and which were set as 100%. The half-lives of the mRNAs (min) are indicated as t½ (bottom). Data are shown above as the mean ± standard deviation of three independent experiments.

Since HS treatment affects many factors other than HuR degradation in cells, we confirmed the HuR-depletion by HuR knockdown (KD) (Figure 2.4). We found that virus propagation was decreased in siRNA-treated cells compared to control siRNA-treated cells (Figure 2.4). Taken together, these results indicate that HuR is essential for Ad-*fos*ARE replication and it replicates in an ARE-mRNA stabilization-dependent manner. Our previous report showed that HuR depletion (HS and HuR KD) causes the downregulation of the replication of WT300 because HuR is required for full replication of adenovirus (Jehung et al., 2017). However, since the downregulation rate of WT300 was lower than that of Ad-*fos*ARE, and this is because the dependency of HuR of Ad-*fos*ARE is significantly higher than that of WT300.

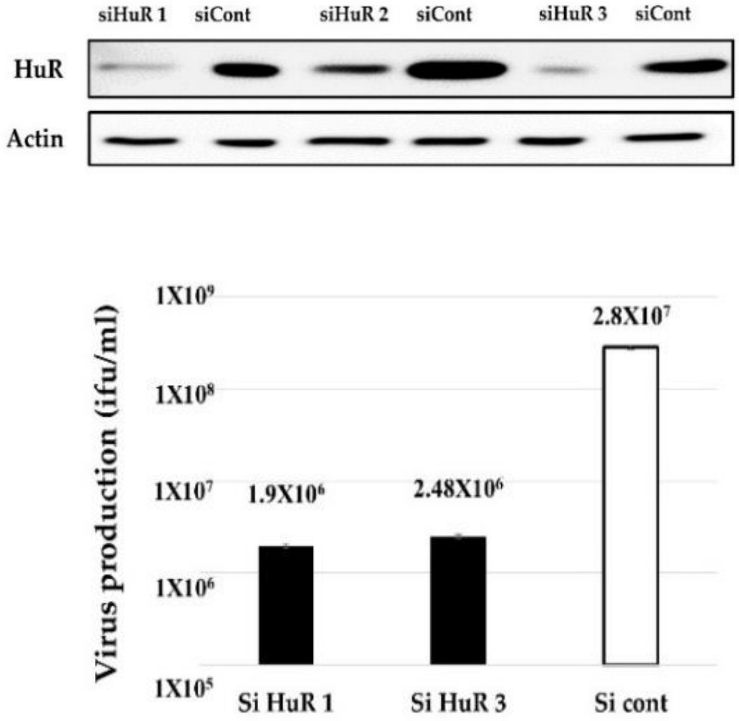


**Figure 2.4.** Effect of HuR knockdown on virus replication. HeLa cells were transfected with a siRNA targeting HuR and a negative control siRNA, and via western blot analysis, the expression of HuR was estimated. (top) HuR KD-HeLa cells were infected with Ad-*fos*ARE, and viral titers were determined as described in materials and methods after 48 h of virus infection. (bottom) Data are shown above as the mean ± standard deviation of three independent experiments.

### 2.3.3. *In vitro* cytolytic potentiality of Ad-*fos*ARE

To estimate the cell lysis activity of Ad-*fos*ARE, we examined cell viability using the XTT assay. Cancer cells (HeLa, A549, U2OS, H1299, C33A, H1299, and HepG2 ) and normal cells (BJ and HGF1) were infected with Ad-*fos*ARE at an MOI of 1,10,100 and 1000 (ifu/cell) and the XTT assay was performed 1, 3, 5 and 7 days after infection (Figure 2.5). Most of the cancer cells died after 7 days in a time-dependent manner. In contrast, most normal cells infected with the virus did not die even after 7 days.

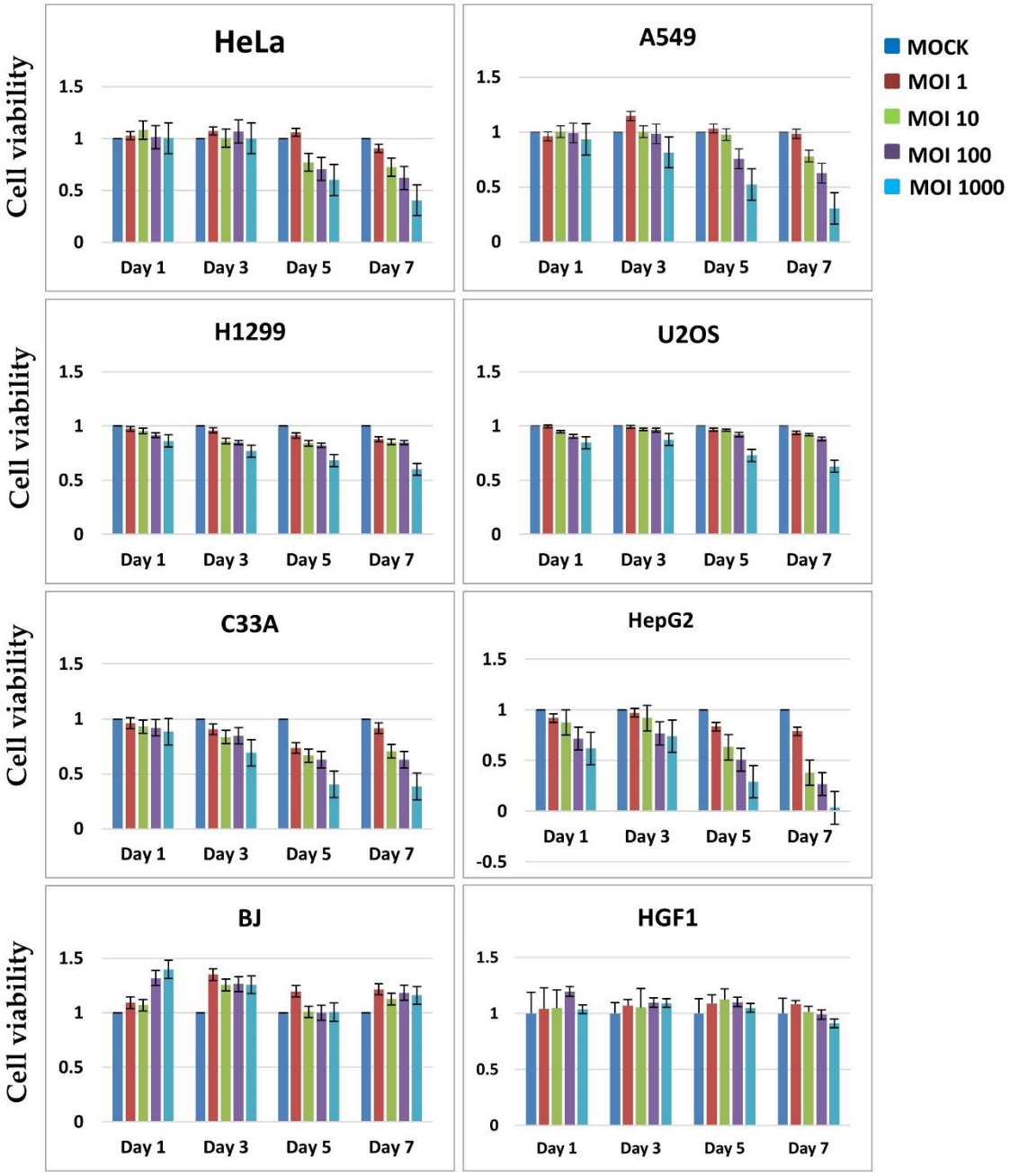


**Figure 2.5.** Cell lysis activity of Ad-*fos*ARE. Cell metabolic activities of Ad-*fos*ARE-infected cells were measured to estimate the cell lysis activity using the XTT assay. Cancer (HeLa, A549, C33A, H1299, U2OS and HepG2) cells and normal (BJ and HGF1) cells were infected with the virus at an MOI of 1,10,100 and 1000 ifu/cell and cell viabilities were estimated 1, 3, 5 and 7 days

post-infection. Data are shown above as the mean ± standard deviation of three independent experiments.

To assess the cell lysis activity of Ad-*fos*ARE further, we examined the cell death of virus-infected cells using a cytopathic effect (CPE) assay. Six different cancer cell lines (HeLa, C33A, A549, H1299, HepG2 and U2OS) and two normal cell lines (BJ and HGF1) were infected with virus at MOIs of 1, 10, 50 or 100 ifu/cell. Cytotoxicity was assessed by staining the remaining cells with Coomassie brilliant blue 7 days after infection (Figure 2.6). The virus killed all cancer cells in a dose-dependent manner, although most normal cells survived in any dose. These results determine the *in vitro* cancer-selective cytolytic activity of Ad-*fos*ARE.

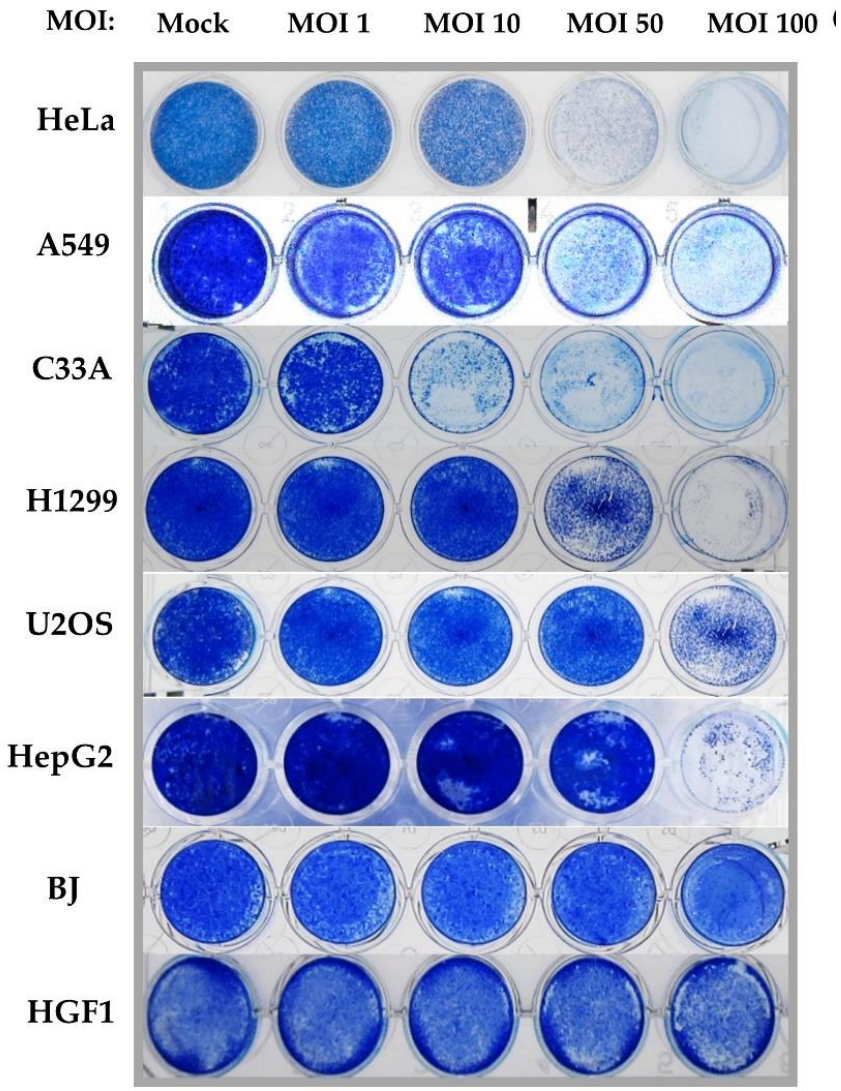


**Figure 2.6.** Cytopathic activity of Ad-*fos*ARE. Cancer (HeLa, A549, C33A, H1299, U2OS and HepG2) cells and normal (BJ and HGF1) cells were

infected with the virus at the MOIs indicated and cells were stained using Coomassie brilliant blue 7 days post-infection. Living cells stained blue.

Next, we explored the pathway behind Ad-*fos*AREF induced cell death in cancer cells. As various pathways of adenovirus-induced cell death such as apoptosis, autophagy has been reported (Abou El Hassan et al., 2004. Tazawa et al., 2017), we examined the proteins expressed specifically for each cell death. Although LC3, expressed autophagy, was not detected in Ad-*fos*ARE infected cells (data not shown), only the processing of the caspase substrate PARP was detected by western blot analysis on various days post-infection (Figure 2.7.A). PARP expression in cisplatin-treated cells was used as a positive control (Anke et al., 2019).

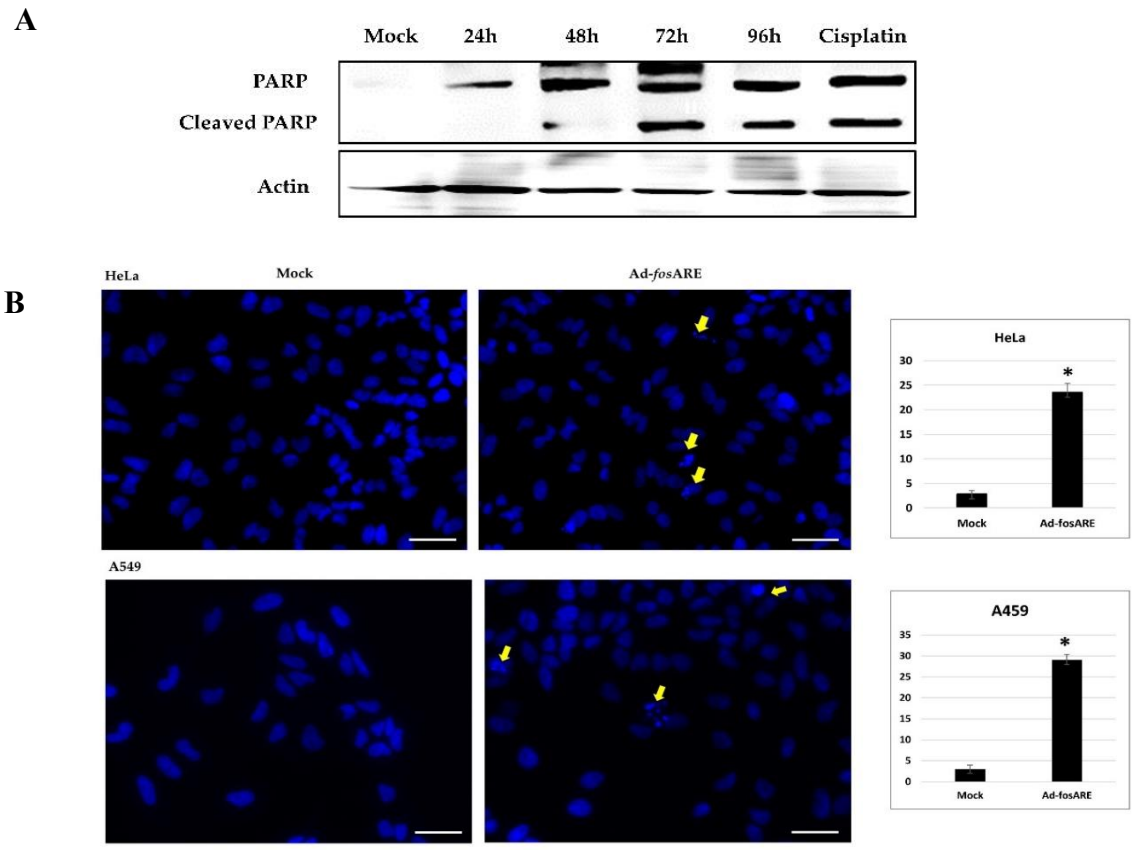


**Figure 2.7.** Assessment of cell death by apoptosis. (A) The expression of the cleavage of PARP was assessed by western blot analysis to detect the cell lysis activity mediated by Ad-*fos*ARE. (B) HeLa and A549 cells were infected with

Ad-*fos*ARE with MOI 100 ifu/cell. 96 h after infection, the apoptosis of cells was also analyzed by Hoechst 33324 staining. Nuclear fragmentation and chromatin clumping were observed in the virus treated cells (Yellow arrows). The number of apoptotic cells was quantitated in the histogram (right panel). Scale bar: 50μm. Three replicates represented each assay.

We also observed the apoptosis by Hoechst 33324 staining. After the cells were infected with the virus with MOI 100 ifu/cell, then cells were stained with Hoechst 33324 to find the morphological changes of cell apoptosis in both control and Ad-*fos*ARE infected cells. Morphological changes of cell apoptosis, such as condensation of chromatin and nuclear fragmentations, were clearly found in Ad-*fos*ARE infected cells (Figure 2.7.B). These results suggest that Ad-*fos*ARE infection-induced apoptosis.

### 2.3.4. Comparison of the oncolytic effects of Ad-*fos*ARE and dl1520

Since an E1B-55k gene deleted-adenovirus dl1520 is already applied clinically (Bischoff et al., 1996; Kasuya et al., 2005), we next compared the oncolytic activity and viral replication of Ad-*fos*ARE with that of the dl1520. Ad-*fos*ARE and dl1520 were infected at an MOI of 10 ifu/cell, using cancer cells, (HeLa, C33A, A549 and H1299) and normal BJ cells, and virus titers were estimated 48 h after infection. As shown in Figure 2.8.A, Ad-*fos*ARE production was higher than dl1520 in all cancer cells. We also compared the cytolytic activity by XTT assay as presented in Figure 2.8.B. Cytolytic activity of Ad-*fos*ARE and dl1520 in cancer cells were more or less similar. But in normal cells, Ad-*fos*ARE caused less damage compared to dl1520.

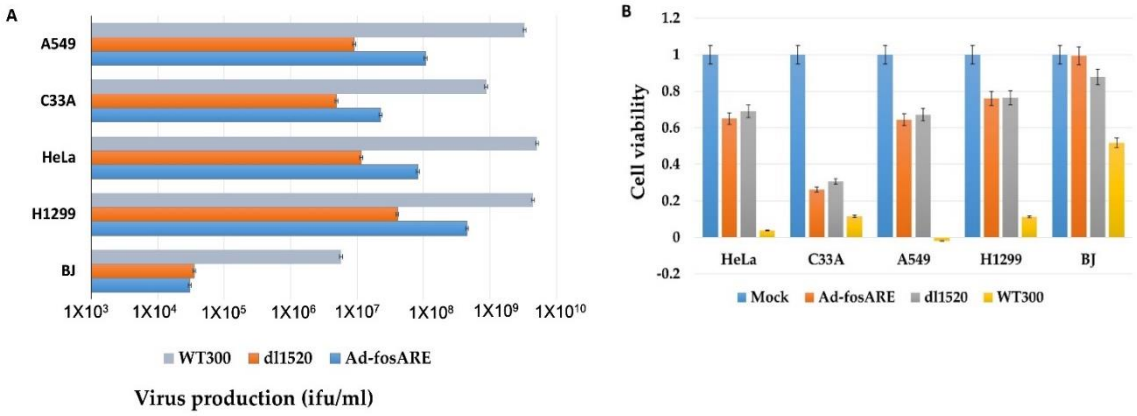


**Figure 2.8**. Comparison of the virus production and cell lysis activity of Ad-*fos*ARE with dl1520 and WT300. (A) Cancer (HeLa, C33A, A549 and H1299) cells and normal (BJ) cells were infected with Ad-*fos*ARE and dl1520 at MOI of 10 ifu/cell. Virus production was assessed 48 h after infection. Each titer (ifu/ml) is shown on the graph. (B) Cell viabilities were estimated 7 days post-infection. Data are shown above as the mean ± standard deviation of three independent experiments.

## 2.4. Discussion

Among the currently investigated oncolytic viruses, the use of oncolytic adenovirus strains appears to be the most promising. In the present study, we demonstrated the oncolytic efficacy of the Ad-*fos*ARE with ARE of the *c-fos* gene, in the 3'UTR of the E1A gene. Our results showed that the replication efficiency of this virus in cancer cells was higher than in normal cells, and also, was better than dl1520 equivalent to H101, which is clinically applied (Bischoff et al., 1996, Kasuya et al., 2005).

We investigated the requirement of mRNA stabilization system for Ad-*fos*ARE replication. Since Ad-*fos*ARE possesses an ARE downstream of *E1A* gene, an increased expression level of E1A mRNA was expected in cancer cells, where ARE-mRNA is stabilized, thereby promoting virus growth. To confirm such ARE-mRNA-dependent virus growth and cell lysis, HuR was depleted by heat shock and knockdown to avoid ARE-mRNA exportation and stabilization. As expected, the virus replication decreased in response to inhibited ARE-mRNA stabilization. Also, the half-life of E1A mRNA was low in HuR-depleted cells compared to control cells. These data indicate that Ad-*fos*ARE replicates in HuR dependent manner. Since, in the vast majority of cancer cells, ARE-mRNAs relocate to the cytoplasm with HuR and are constitutively stabilized (López et al. 2003), these facts suggest that Ad-*fos*ARE has the potential to be effective for many types of cancer cells.

In a previous study, an adenovirus including the ARE of *COX-2* gene in the 3'-UTR of the *E1A* gene was shown to be a conditionally replicating virus (Ahmed et al., 2003) and that virus replicated selectively in RAS/P-MAPK-activated cancer cells because ARE-mRNA was stabilized under the activated RAS pathway. In the case of Ad-*fos*ARE, cytolytic activity was not dependent on the RAS/P-MAPK pathway, because the virus exhibited oncolytic activity for HeLa cells, which carry a normal *ras* gene. These findings indicate that Ad-*fos*ARE is effective for cancer cells carrying unmutated *ras*. These data indicate that Ad-*fos*ARE is effective in more cancers than previously shown viruses.

Since the stability of ARE-mRNA has been reported in many biological or pathological events, such as inflammation, viral infection, hypoxia, and UV irradiation, Ad-*fos*ARE has potential in the treatment of diseases with these biological features.

# Chapter III

# Synergism of Oncolytic Adenovirus Utilizing RNA Stabilization Mechanism and Paclitaxel

## 3.1 Introduction

Oncolytic adenovirus can be used either as a standalone therapeutic modality or in combination with other approaches to overcome or enhance viral activity in the tumor microenvironment. Paclitaxel (PTX) is the most common anticancer agent used against many cancers, but the emergence of drug resistance is a major drawback. PTX is a microtubule (MTs) stabilizing drug (Ingemarsdotter et al., 2010; McGuire et al., 1996) and inhibits cell replication by enhancing the polymerization of tubulin monomers into stabilized microtubule bundles that are unable to reorganize into the proper structures during mitosis (McGuire et al., 1996; Horwitz et al., 1992). MT networks are very important for adenovirus entry, nuclear trafficking, development of replication compartments, and controls broader aspects of infected-cell behavior (Kelkar et al., 2004). After entering through the receptor, the viral capsid interacts with the motor protein dynein and trafficking to the nucleus in a microtubule-dependent manner (Leopold et al., 2007). Virus infection and consequent signaling alter the MT dynamics of the host cell, thus making MTs stable for the intracellular transport of the virus (Warren et al., 2016).

PTX can increase the expression of coxsackie and adenovirus receptor (CAR) (Seidman et al., 2001; Fok et al., 2007). Adenoviral fiber knob of the capsid binds with cell surface receptor CAR and initiates gene transfer (Abdolazimi et al., 2007). CAR is a 46-k transmembrane glycoprotein and belongs to the immunoglobulin superfamily, which is the primary receptor for adenovirus (Abdolazimi et al., 2007; Tomko et al., 1997; Bergelson et al., 1997). Furthermore, PTX increases the HuR export to the cytoplasm in cancer cells and thus facilitates mRNA stabilization (Badawi et al., 2018). Some studies have shown that the ubiquitously expressed HuR can utilize either the actin- or microtubule-dependent cytoskeleton for the transport of mRNA cargo (Cheng et al., 2013; Doller et al.,2008; Holt et al., 2008). MTs are essential for cell motility and the transport of organelles like; vesicles and are relevant for long-distance transport of protein and mRNA (Holt et al., 2008; Blower et al., 2013; Eberhardt et al., 2016).

In this study, I show that Ad-*fos*ARE can synergies with a microtubule stabilizer PTX. Use of heat shock or a knockdown depleted HuR, which further down-regulated Ad-*fos*ARE replication was indicating that Ad-*fos*ARE replicates in an ARE-mRNA stabilization-dependent manner. PTX promotes the nuclear export of HuR, which can

enhance the propagation of Ad-*fos*ARE, in cancer cells but not in normal cells. Furthermore, it up-regulated the expression of CAR and increases virus internalization. The oncolytic activity of Ad-*fos*ARE was enhanced synergistically by PTX through the increase of E1A expression and enhancement of viral apoptotic activity both *in vitro* and *in vivo*. These results indicate that PTX offers many benefits to Ad-*fos*ARE.

## 3.2 Materials and method

### 3.2.1 Cell Lines

A549 (human lung cancer cell line) and HeLa, HeLa S3 (human cervical carcinoma cell lines), 293 (human embryonal kidney cells transformed by the adenovirus E1 gene) and BJ (human foreskin fibroblast cell line) were used in this study. Cells were acquired from the American Type Culture Collection (ATCC; Manassas, VA, USA) and cultured in Dulbecco's modified Eagle's medium (DMEM; Sigma-Aldrich; Merck KGaA, Darmstadt, Germany) including 10% fetal bovine serum (FBS; Biowest, Nuaille, France) with antibiotics at 37 °C in a 5% $CO_2$ atmosphere in humidified conditions.

### 3.2.2 Cytopathic effect (CPE) assay and cell viability assay

Cancer and normal cells were seeded on 24-well plates ($5\times10^4$ cells/well). 24 h later, the cells were treted with PTX (4 nM) and, additional 4 h after, they were infected with Ad-*fos*ARE at a multiplicity of infection (MOI) of 1, 10 ,50, and 100 ifu/cell and maintained for an additional 7 days. Then cells were fixed and stained with Coomassie brilliant blue.

A 2-3-bis [2-methoxy-4-nitro-5-sulfophenyl]-2H-tetrazolium-5-carboxanilide inner salt assay was used to observe the cytolytic activity. Cells were seeded on 96-well plates at $3\times10^3$ cells/well. 24 h later, the cells were treted with PTX (4 nM) and, additional 4 h after, they were infected with Ad-*fos*ARE at a MOI of 10 ifu/cell. Cytolytic activity was assessed using an XTT assay on days 1, 3, 5, and 7 with the Cell Proliferation kit II (Roche Diagnostics, Basel, Switzerland) according to the manufacturer's protocol.

### 3.2.3 Western blot analysis

Cells were treated with 4 nM PTX and were lysed with RIPA buffer (150 mM NaCl; 25 mM Tris-HCl, pH 7.6; 1%Nonidet P-40; 1% sodium deoxycholate; 0.1% SDS) containing protease inhibitors. Equal amount (20 µg) of total protein were separated by 10% sodium dodecyl sulfate-polyacrylamide gel electrophoresis (SDS-PAGE) and transferred onto polyvinylidene difluoride membranes (Millipore, Billerica, MA, USA). Fractionation buffer (10 mM Tris-HCl, pH 7.6, 150 mM NaCl, 1.5 mM $MgCl_2$, 0.5% Nonidet P-40, protease inhibitor cocktail) was used to fractionate the cytoplasmic and nuclear proteins, followed by vigorous shaking for 5 min and centrifugation at 12,000 rpm for 30 s. The supernatant was used as the cytoplasmic protein fraction. To assess the accuracy of cell fractionation, cytoplasmic (β-tubulin) and nuclear (lamin B) proteins were detected. For detection of surface protein CAR, the protocol described in Andolazimi *et al*., was used (Andolazimi et al., 2007).

### 3.2.4 Immunocytochemistry

HeLa, A549 and BJ Cells were grown on coverslips in 35-mm dishes at 60–80% confluence and treated with PTX (4 nM) for 4 h. Immediately following the treatment, cells were rinsed once with phosphate buffer saline (PBS), fixed for 20 min at room temperature with 4% paraformaldehyde in PBS, blocked and permeabilized in 2% BSA plus 0.1% Triton X-100 in PBS at room temperature. Subsequently, the fixed cells were incubated with HuR and Tubulin (abcam 6160) primary antibody for overnight at 4 °C followed by Alexa Fluor 488 and Alexa Fluor 568 secondary antibodies for 1 h at room temperature respectively. Cell nuclei were counterstained with DAPI.

For Hoechst 33342 staining, cells were infected with Ad-*fos*ARE (MOI 10 ifu/cell) and treated with PTX (4 nM). After these treatments, cells were rinsed once with phosphate buffer saline (PBS), fixed for 20 min at room temperature with 4% paraformaldehyde in PBS, blocked and permeabilized in 2% BSA plus 0.1% Triton X-100 in PBS at room temperature. Cell nuclei were stained with Hoechst 33342 before mounted on slides by using Mountant permafluor (Thermo scientific, FM 111212A). Cells were observed using an IX71 inverted microscope (Olympus). Image acquisition was performed with the Olympus FluoView Software (FV10-ASW Viewer, ver.4.2).

### 3.2.5 *In vitro* virus proliferation assay

Cancer cells and normal cells were seeded into 12-well plates at a density of $5\times10^4$ cells/well 24 h before the infection. After 4 h of treatment of PTX (4 nM), cells were infected with Ad-*fos*ARE at an MOI of 10 ifu/cell, and the medium was not changed after virus infection. After incubation at 37 °C for 72 h, cells were collected, and a virus lysate was prepared as described above. Viral titers (ifu/ml) were determined using the Adeno-X Rapid Titer kit (Clontech Laboratories). For virus exit assay, the medium was collected from virus-infected cells and centrifuged for 5 min at 4000 rpm then the supernatant was tittered (Ingemarsdotter et al., 2010).

### 3.2.6 RNA extraction and quantitative RT-PCR

Total RNA was extracted using the RNeasy Mini Kit (250) from QIAGEN and the RNA was subjected to reverse transcription by ReverTra Ace qPCR RT master mix with genomic DNA remover (Toyobo, Osaka, Japan). Quantitative RT-PCR was performed in the DNA Engine Opticon2 (MJ Research, Watertown, MA, USA), and cDNA was amplified using the following primers: Ad5 E1A; 5'-gaa cca ccta ccc ttc acg-3', 5'-ccg cca aca tta cag agt cg-3', GAPDH; 5'-atc ctg ggc tac act gag ca-3', 5'-tgc tgt agc caa att cgt tg-3'. GAPDH was used for normalization. To evaluate the E1A mRNA, HeLa cells were infected with Ad-*fos*ARE, WT300 and treated with PTX for 24, 48, 72 and 96 h and cellular RNA of each cell was used for quantitative RT-PCR. To estimate the half-life of total E1AmRNA, cells were treated with 5μl/mL Actinomycin D 60, 120, or 180 min. The total cellular RNA of each cell was used for quantitative RT-PCR.

### 3.2.7 *In vivo* analysis

Female BALB/c nu/nu mice (5-week-old and 20-22 g) were purchased (Hokudo, Sapporo, Japan) and kept in a specific pathogen-free environment. The temperature was maintained at 26-28 °C, 10 h/14 h light/dark cycle; food and water were given *ad libitum*. Flank tumor was established by injecting HeLa S3 cells ($1\times10^6$ cells/mouse) subcutaneously into the flanks of mice and permitted to grow to ~5-6 mm in diameter. The mice were assigned into four groups randomly (five per group) and PTX (0.4 mg/100 μl) or vehicle (cremophor EL/dehydrated ethanol/saline) was given by intraperitoneal (i.p) injection. $1\times10^6$ ifu (100 μl) of Ad-*fos*ARE or the same volume of PBS was injected intratumorally (i.t) thrice (days 1, 4, and 7) after PTX injection. The

perpendicular diameters of the tumors were recorded every 2 or 3 days. Tumor volumes were measured using the following equation: Volume ($mm^3$) = $A \times B^2 \times 0.5$ (A is considered the longest diameter, B is considered shortest diameter). The body weight and motor activity of each animal was monitored as indicators of general health and toxicity. The mice were sacrificed by cervical dislocation after 21 days of injection of the virus as the tumors on the control group began to ulcerate. All techniques executed in this study involving animals were performed according to the ethical standards of Animal Care and Use Committee of the Hokkaido University. Sapporo, Japan (Permission number for the animal experiment: 19-0099).

### 3.2.8. Immunohistochemistry

The xenografted tumors were removed, fixed with 4% formaldehyde, and embedded for hematoxylin & eosin staining and immunohistochemistry. Next paraffin-embedded specimens were sectioned in 4-µm-thick. The immunohistochemical detection of Adenovirus 5 (Abcam, ab6982) was performed using anti-Adenovirus Type 5 (Rabbit Adenovirus antibody, dilution, 1:1,000; catalog no.,ab6982; Abcam) in PBS in a humidified chamber at 4 °C overnight. The sections were then subjected to anti-rabbit secondary antibody (H1901, Nichirei Bioscience, Tokyo, Japan) at 37 °C for 30 min, followed by antibody detection using a peroxidase conjugated streptavidin-diaminobenzidine (DAB) readout system (DAKO), and counterstaining with DAPI. Rinses were carefully performed with several changes of PBS between each stage of the procedure (5 min washes repeated three times). Images were randomly captured using a nanozoomer slide scanner and NDPViewer (NanoZoomer 2.0 HT, version 2.3.27, Hamamatsu, Shizuoka, Japan).

## 3.3 Results

### 3.3.1 The potentiality of paclitaxel for synergism

It is reported that low concentration PTX increases the cytoplasmic exportation of HuR (36kDa) (Badawi et al., 2018), so we examined whether a low dose of PTX (4 nM) induces the cytoplasmic HuR exportation, as the upregulation of the cytoplasmic HuR expression has to benefit for the replication of Ad-*fos*ARE. We treated cancer cells with PTX and incubated for 4, 8 and 24 hours and collected and fractionated the cytoplasmic and nuclear protein. We found an increase in cytoplasmic HuR exportation in cancer cells by western blot analysis (Figure 3.1.A). Normal cells BJ were also treated with PTX and checked by western blot analysis, but after 24 hours of treatment, cytoplasmic HuR were decreased contrary. HuR exportation was also confirmed using confocal microscopy. HuR localization PTX treated HeLa, A549 and BJ cells was observed using immunostaining method. In cancer cells, cytoplasmic HuR increased in the PTX treated cells compared to control cells (Figure 3.1.B). But in the case of normal cells BJ, PTX treatment diminished cytoplasmic HuR compared to control cells. These results indicate that PTX has the potential to increase cytoplasmic HuR in cancer cells but not in normal cells.

**A**

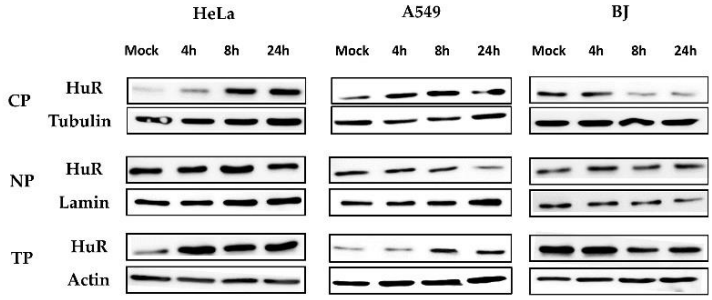
HeLa
A549
BJ
Mock 4h 8h 24h
Mock 4h 8h 24h
Mock 4h 8h 24h
CP
HuR
Tubulin
NP
HuR
Lamin
TP
HuR
Actin

**B**

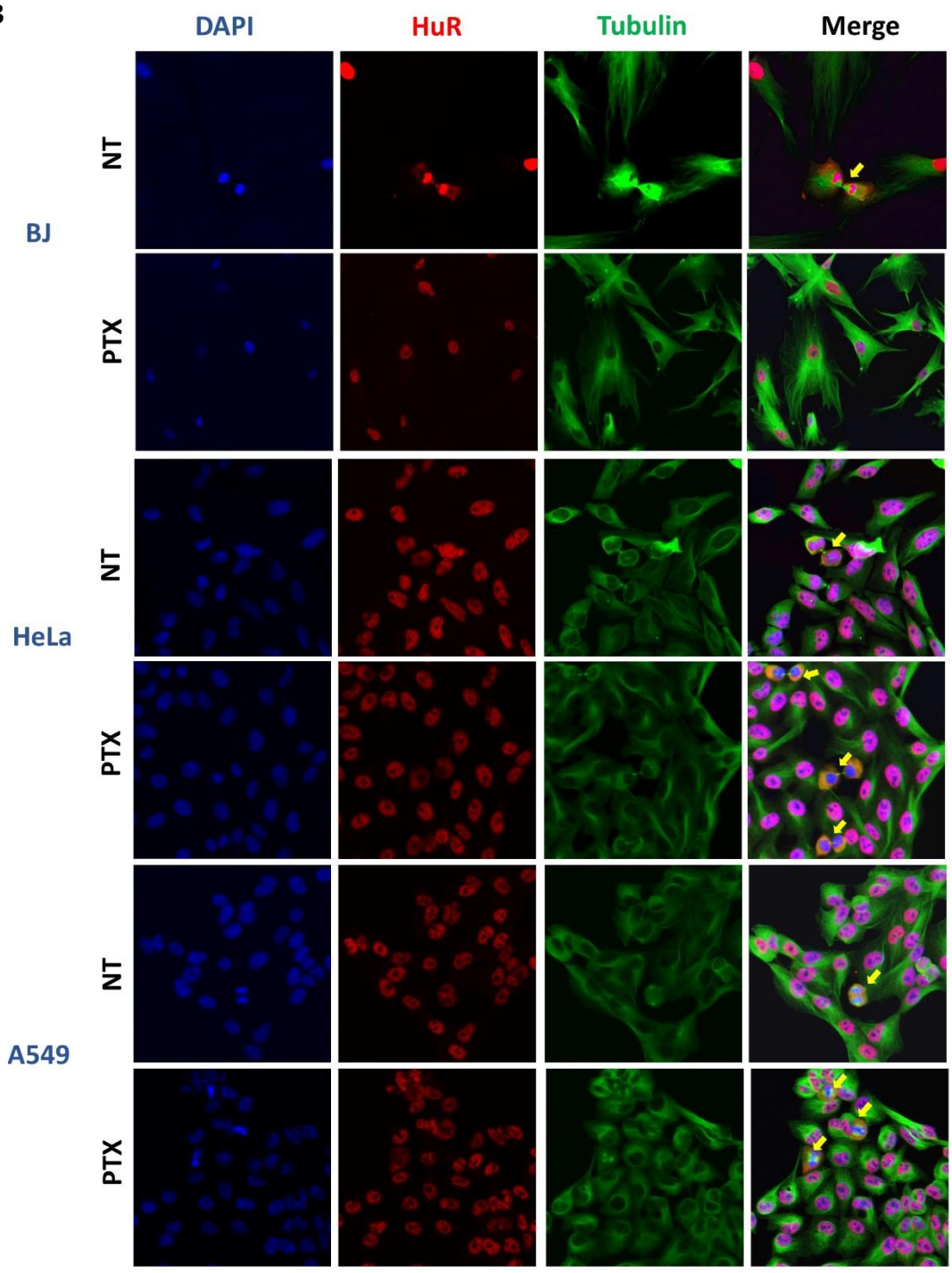
DAPI
HuR
Tubulin
Merge
BJ
NT
PTX
HeLa
NT
PTX
A549
NT
PTX

**Figure 3.1**.Effects of paclitaxel on cytoplasmic HuR exportation. (A) Cancer (HeLa and A549) cells and normal (BJ) cells were treated with 4nM PTX. Cells were separated into the cytoplasmic and nuclear fractions and HuR localization was estimated by western blot analysis. The level of HuR protein was monitored in total cell lysates (TP) and cytoplasmic (CP) and nuclear extracts (NP). Tublin, Lamin and Actin are the inner control of each fraction. (B) Confocal microscopy was performed to visualize changes in HuR exportation. HeLa, A549 and BJ cells were treated with PTX (4 nM) and were stained with HuR and Tublin after fixation and permeabilization as described in materials and methods. In all cases, cell nuclei were visualized by staining with DAPI. Bars indicate 20 μm. Data shown are from a single experiment representative of three repeats giving similar results.

Coxsackie-adenovirus receptor (CAR), which is the primary affinity receptor for adenovirus also upregulated by PTX . The first interaction of adenovirus with cells occurs through the virus fiber protein with its cell surface receptor CAR. This binding leads to internalization of the virus by endocytosis and trafficking along dynein (motor protein of microtubules) toward the nucleus (Seidman et al., 2001; Fok et al., 2007). To check the CAR (46kDa) expression, HeLa cells were treated with 4nM PTX for a different time course, and after treatment, CAR expression was examined by western blot analysis. As shown in Figure 3.2, CAR expression increased after treatment with PTX.

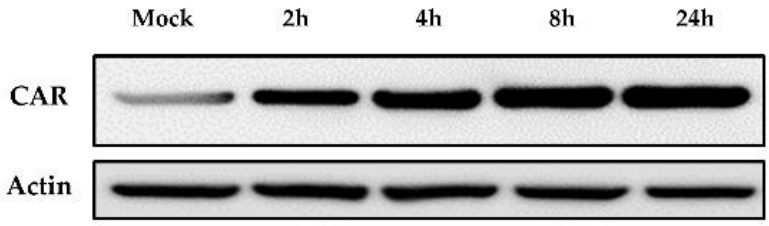


**Figure 3.2.** Western blot analysis of expression of coxsackie-adenovirus receptor (CAR) at different time-points. After treatment with PTX, total HeLa

cell lysate was collected and CAR expression was analysed by western blot analysis.

### 3.3.2 Synergistic effect of oncolytic adenovirus and PTX

To explore the potential relationship between Ad-*fos*ARE and chemotherapy, we determine the virus propagation after combination treatment. HeLa, A549 and BJ cells were treated either with the virus only or a combination of drug and virus. Virus titers generated after 48 h were detected by staining the hexon protein. We found that after combination treatment virus titer increases to 10 fold in cancer cells but no significant changes in normal cells (Figure 3.3.A).

XTT assay was executed 1, 3, 5 and 7 days after Ad-*fos*ARE infection using HeLa, A549 and BJ cells (Figure 3.3.B). In the case of cancer cells, although cell viability by PTX or virus alone was not changed, the combination with 4 nM PTX and virus (MOI 10) resulted in reduced it 5 days after infection and most cells died after 7 days. However, in the case of normal BJ cells, no synergistic effect was found. Although both HeLa and A549 cells showed dose-dependent cytotoxicity after exposure to PTX, A549 cells were slightly more sensitive than HeLa cells. Combination index for HeLa ranging from 0.5-0.85 and A549 ranging fron 0.40-0.52 was calculated using Chou-Talalay equations and analyzed by Compusyn (Supplementary Figure 2). A CI of <0.9 indicates synergism and a CI between0.9, and 1.1 measured additive effect, whereas a CI of >1.1 indicates antagonistic (Chou 2010).

We also performed the cytopathic effect of the combination approach. First, we treated the cells with PTX for 4 h and subsequently infected them with the virus. After 7 days post-infection, we observed almost all cells were killed with combination treatment, which suggests a synergistic effect rather than the cumulative effect (Figure 3.3.C). Moreover, in the normal cell, no impact of the combination was present. Taken together, these results indicate that PTX can enhance the activities of Ad-*fos*ARE and suggests the synergistic effect of Ad *fos*ARE with PTX.

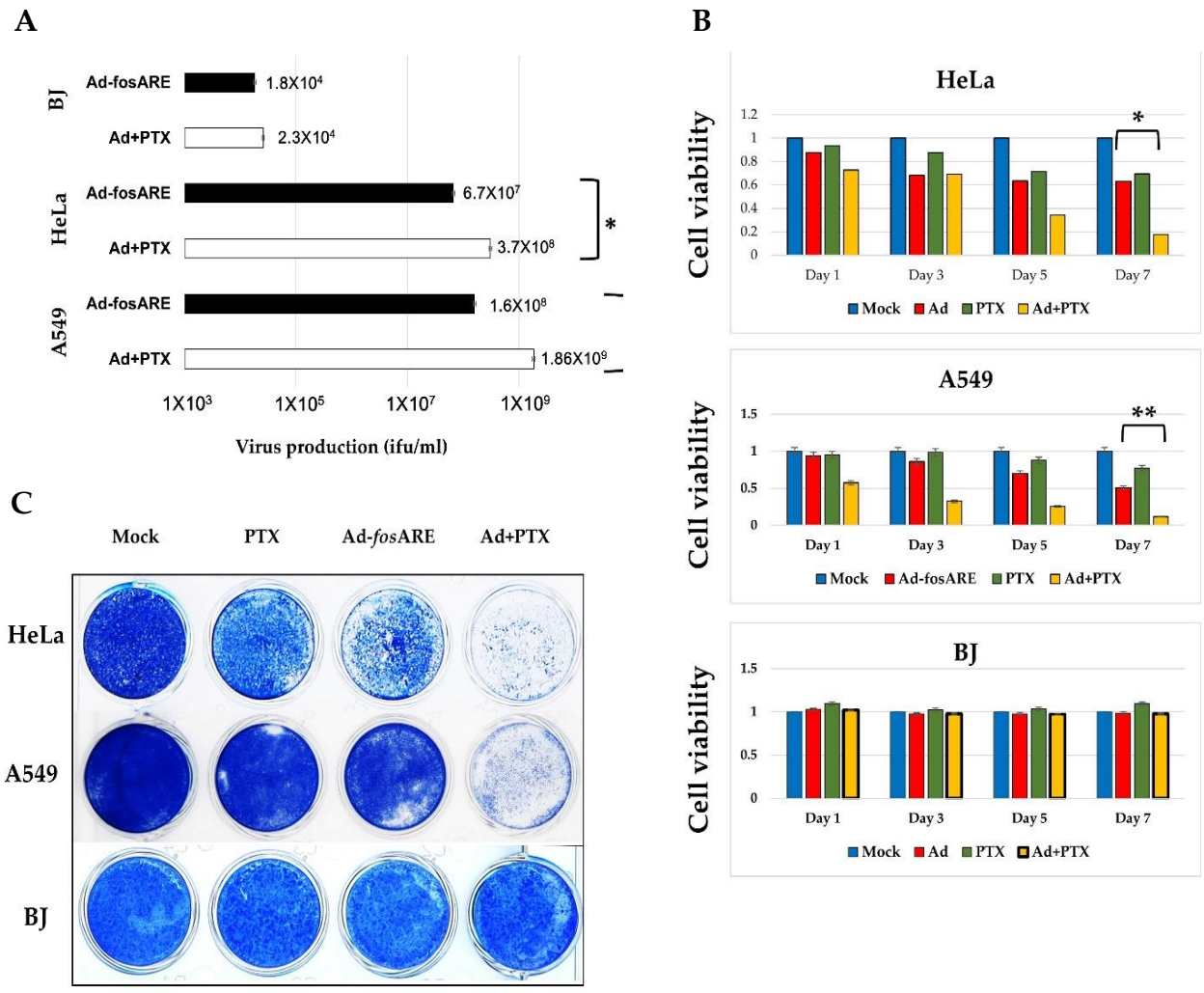


**Figure 3.3.** Assessment of combinatorial treatment's effect (Ad-*fos*ARE and PTX) on viral replication and cell lysis activity. (A) Cancer (HeLa and A549 ) cells and normal (BJ) cells were infected with Ad-*fos*ARE at an MOI of 10 ifu/cell and 4nM PTX. Virus production was determined 48 h after by hexon staining. Each titer (ifu/ml) is shown on the graph. Data are shown above as the mean ± standard deviation of three independent experiments. (B) Cell lysis activities of combination treatment were measured using the XTT assay. Above mentioned cancer and normal cells were infected with the virus at an MOI of 10 ifu/cell and cell viabilities were estimated 1, 3, 5 and 7 days after infection. (C) Same cancer and normal cells were subjected to obbserve cytopathic effects. Cells were stained using Coomassie brilliant blue 7 days after infection. Living cells stained blue. (* indicates $p<0.05$, ** $p<0.01$)

### 3.3.3 Effects of PTX on Ad-*fos*ARE viral proteins expression and E1A mRNA stabilization

The effect of paclitaxel on viral protein synthesis was assessed by western blot analysis. HeLa and A549 cells were treated for 72 h with only virus and combination, and then total cell lysate was analysed to detect E1A (30~50 kDa) and E1B-55k. Quantification of the western blot results shows that there were significant changes of E1A protein synthesis in combination treatment whreas almost no changes were observed in E1B-55k expression (Figure 3.4).

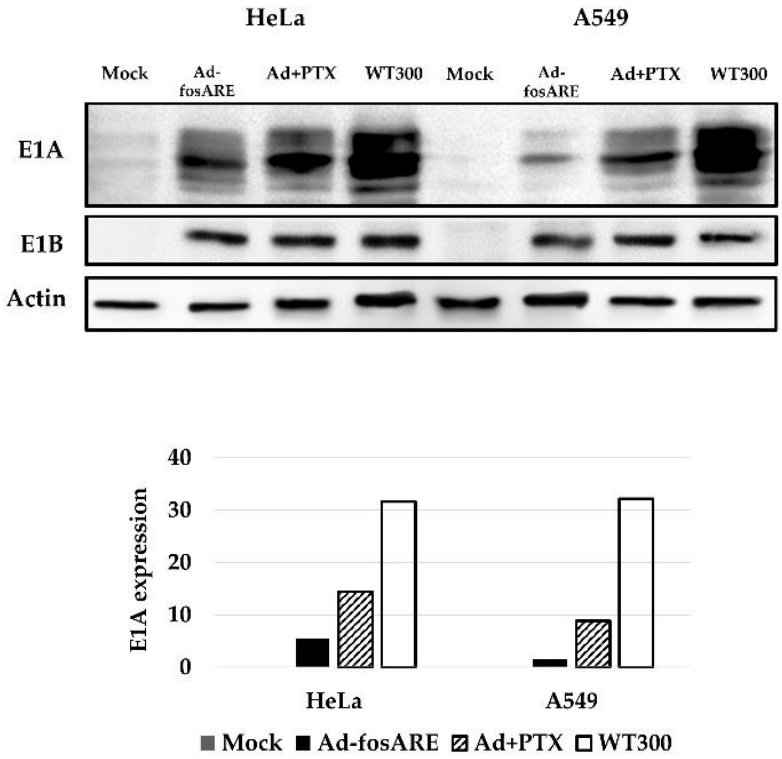


**Figure 3.4.** Effects of PTX on the expressions of Ad-*fos*ARE proteins. To check the viral protein synthesis, HeLa and A549 cells were treated in combination with Ad-*fos*ARE (MOI 10) and PTX (4 nM). E1A and E1B-55k were estimated by western blot analysis (Top). Densitometric data of E1A expression is shown (bottom).

We also examined the E1A mRNA expression by real-time RT-PCR, and the results were in line with western blot results as the E1A mRNA expression was significantly higher in combination treatment after 72 h of treatment (Figure 3.5.A). Also the half-life of ARE including E1A mRNA transcribed from Ad-*fos*ARE was prolonged by PTX treatment from 239 to 517 minutes. On the other hands, E1A mRNA without ARE synthesized by WT300 was changed from 80.9 to 99 minutes (Figure 3.5.B). These data suggest that PTX enhances Ad-*fos*ARE replication through stabilization of ARE containing E1A mRNA.

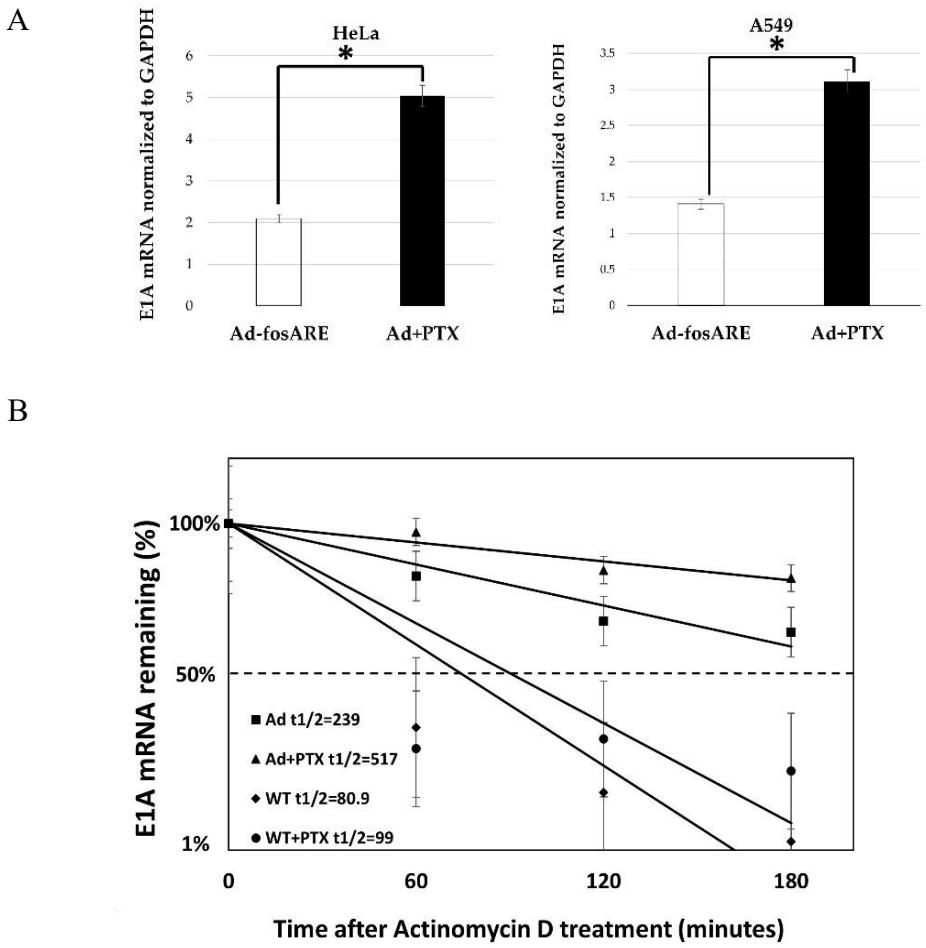


**Figure 3.5.** Effects of PTX on E1A mRNA trabscribed from Ad-*fos*ARE. (A) HeLa and A549 cells were treated in combination with Ad-*fos*ARE (MOI 10) and PTX (4 nM). E1A mRNA was detected by quantitative real-time RT-PCR using GAPDH mRNA as a normalized control. (B) E1A mRNA stabilization

in Ad-*fos*ARE infected cells. HeLa cells were infected with Ad-*fos*ARE (MOI 10 ifu/cell) and combination with PTX. Transcriptions were blocked by actinomycin D 5µl/mL for 60, 120 and 180 minutes. After the indicated periods, cells were harvested and extracted for total cellular RNA. mRNA levels are quantified by quantitative real-time RT-PCR using GAPDH as a normalization control. Graphs depict the percentage of remaining E1A mRNA levels with GAPDH mRNA and compared with the standards of normalized mRNA species measured immediately after the addition of actinomycin D and which were set as 100%. The half-lives of the mRNAs (min) are indicated as t½. Data are shown as the mean ± standard deviation of three independent experiments (* indicates $p < 0.05$).

### 3.3.4 Combination treatment Increases the Level of Posttranslationally Modified Tubulin

We also examine whether Ad-*fos*ARE can affect the mechanisms of paclitaxel activity by upregulating-acetylated α-tubulin, which is the marker for stabilized microtubules (Warren et al.,2006). After quantifying the western blot analysis data shows the level of acetylated α-tubulin increased with combination treatment by 48 h (Figure 3.6.A). Alteration of the dynamic instability of MTs is essential for virus trafficking to the nucleus. Virus infection causes modulation of MT dynamics by Posttranslationally modified MTs through a RhoA-dependent mechanism. Posttranslationally modified MTs are detyrosinated (Glu-MTs) and acetylated MTs. Results show that both Glu-MTs and acetylated α-tubulin was higher in combination treatment (Figure 3.6.A, Supprementaly Figure 4).

### 3.3.5 Virus exit assay

The changes in posttranslationally modified MTs by the virus are transient, so we next determined whether MTs stabilization by PTX affected viral exit or release from cells (Figure 3.6.B). In the case of the combination treatment, free virus release was higher than treated with the only virus, which indicate PTX does not interfere with virus release. Intracellular viral replication was also measured by tittering the attached cells, and the result shows viral replications were also higher in combination-treated cells (Supprementaly figure 5). Figure 3.3.B shows there was no difference in cell lysis activity between only virus treated and combination treated HeLa cells on 72 h. So,

from the results of virus exit assay we can assume that the virus can be released from the intact cells by a microtubule-dependent pathway.

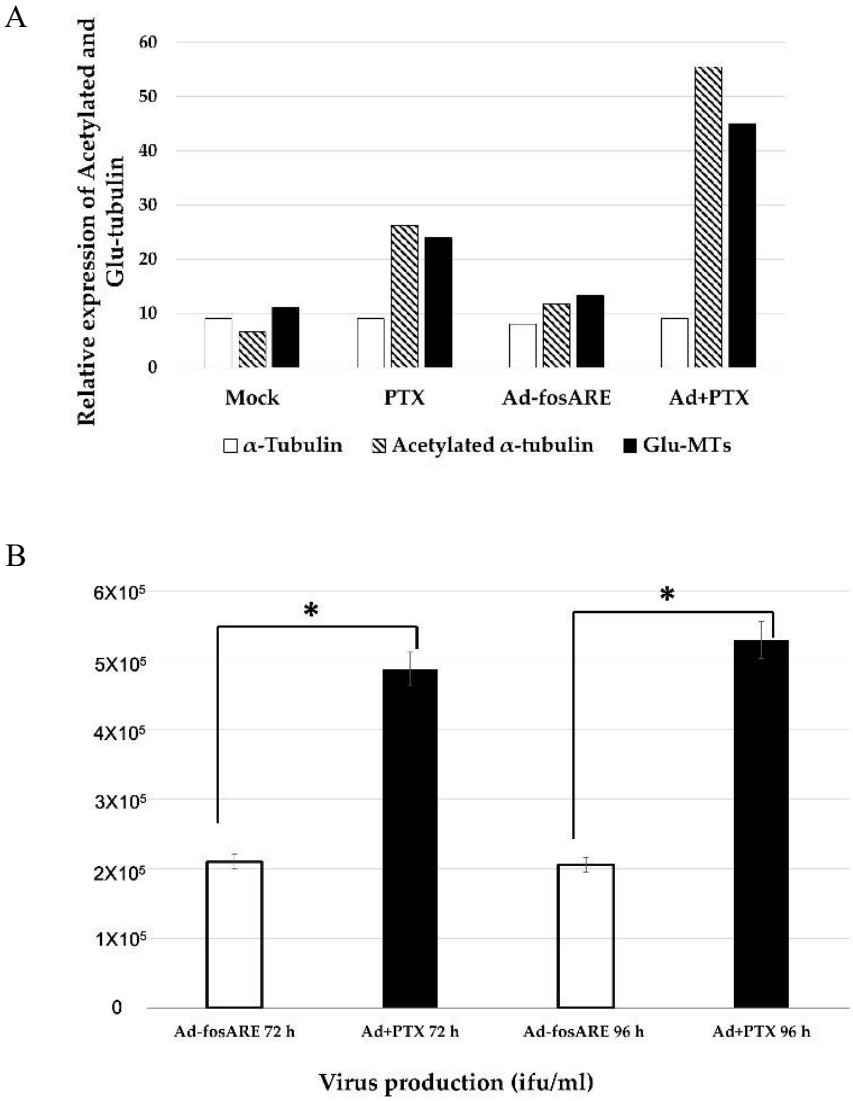


**Figure 3.6**. Effects of paclitaxel on tubulin modifications and Ad-*fos*ARE exit. (A) To determined posttranslationally modified tubulin, HeLa cells were treated with Ad-*fos*ARE, PTX and combination. The expression of acetylated and Glu-MTs was quantified by densitometry and the values were normalized to non-infected conditions. (B) For virus exit assay, HeLa cells were treated with 4nM PTX and infected with an MOI of 10 ifu/cells of Ad-*fos*ARE. The supernatants were tested for viral particles 72 and 96 h after infection. Data are shown above as the mean ± standard deviation of three independent experiments (* indicates $p < 0.05$).

### 3.3.6 Effects of paclitaxel on the cell lysis activity of the virus

To determine the combined effect of paclitaxel and virus on cell death, we examined the levels of caspase substrate PARP (116 kDa) and cleaved PARP (89 kDa) (Figure 3.7.A). HeLa cells were treated and the whole lysate was collected after 96 h and subjected to western blot analysis. Both full length and cleaved PARP were found in combination treatment just like the positive control.

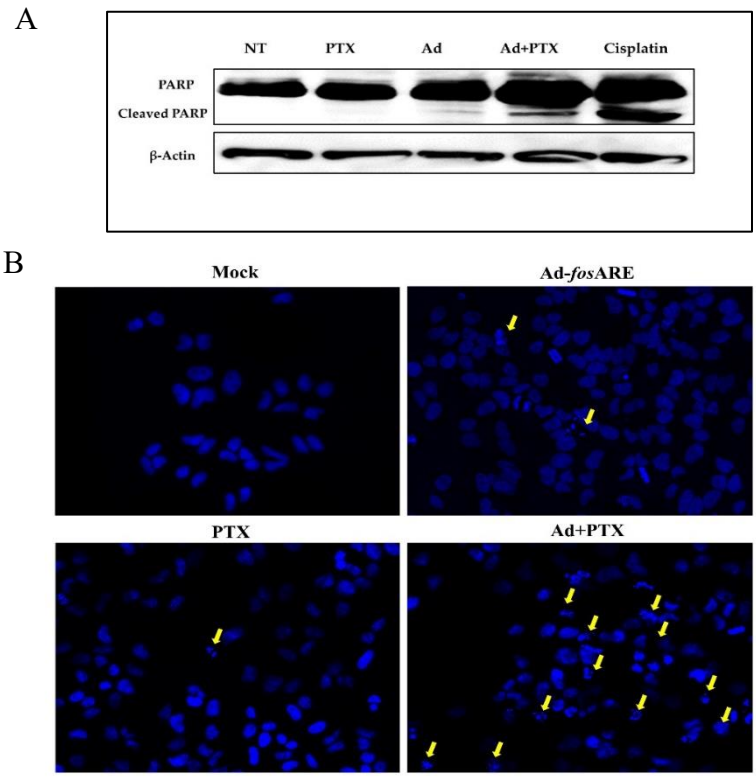


**Figure 3.7.** Apoptotic cell death induction of Ad-*fos*ARE infected cells by PTX. (A) The expression of the cleavage of PARP was assessed to detect the cell lysis activity by combination treatment. HeLa cells were infected with the virus, PTX and combination and whole-cell lysate were subjected to western blot ananlysis. The cisplatin-treated lysate was used as a positive control. (B) HeLa cells were treated with PTX (4 nM) and 4 h after treatment, Ad-*fos*ARE was infected at an MOI 10 ifu/cell. The apoptosis of cells was also analyzed by Hoechst 33324 staining 96 h after infection,. Yellow arrows indicate nuclear fragmentation and chromatin clumping. Scale bar:50μm.

To investigate the apoptotic cell death further, HeLa cells treated with Ad-*fos*ARE or PTX or combination were stained with Hoechst 33342 to observe apoptotic bodies, chromatin condensation, and nuclear fragmentation. As shown in Figure 3.7.B, combination treatment resulted in significantly increased these apoptotic features compared to Ad-*fos*ARE or PTX treatment alone. Taken together, these results indicate that PTX enhanced the apoptosis of the cancer cells infected with Ad-*fos*ARE.

### 3.3.7 *In vivo* synergistic effect of Ad-fosARE and Paclitaxel in murine flank tumor

In order to examine *in vivo* effects of Ad-*fos*ARE, a flank tumor model of human HeLa cervical cancer in 5-week-old female BALB/c nu/nu mice was used to study the consequence of Ad-*fos*ARE and PTX therapy. Once the tumors had reached ~5-6mm in diameter, they were treated with the equitable volume of PBS, Ad-*fos*ARE, PTX or combination. The combination of Ad-*fos*ARE+PTX showed a significantly reduced mean tumor volume ($\pm$ 27 $mm^3$) compared to Ad-*fos*ARE alone ($\pm$ 57 $mm^3$), PTX alone ($\pm$ 124 $mm^3$) or control ($\pm$ 240 $mm^3$). Tumors treated with the combination had a smaller mean volume compared to only Ad-*fos*ARE, only PTX and control (Figure 3.8). The study was terminated when the tumors of the control group began to ulcerated. No morbidity attributable to either tumoprogression or therapy was observed. These results indicate *in vivo* synergistic effect of Ad-*fos*ARE and PTX.

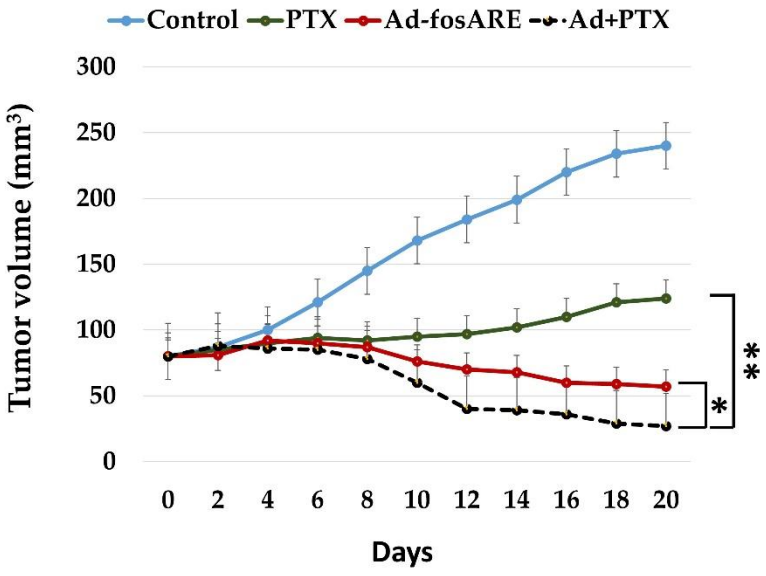

**Figure 3.8.** *In vivo* tumor lysis potential of the combination therapy of Ad-*fos*ARE and PTX in human cervical cancer xenograft nude mice. HeLa S3 cells were injected subcutaneously into the flanks of female BALB/C nude mice and allowed to grow to ~5-6 mm in diameter. PTX (0.4 mg/100µl) or vehicle (cremophor EL/dehydrated ethanol/saline) was given by intraperitoneal (i.p.) injection. $1X10^6$ ifu (100 µl) of Ad-*fos*ARE or the same volume of PBS was injected intratumoral (i.t.) thrice (days 1, 4 and 7) directly into the tumors after PTX injection. Tumor volumes were calculated by the following equation: Volume ($mm^3$) = A x $B^2$ x 0.5 (A is considered longest diameter, B is considered shortest diameter). * indicates $p < 0.05$, **$p < 0.001$.

### 3.3.8. PTX induces in vivo virus propagation.

To assess the *in vivo* cytolytic effect of Ad-*fos*ARE, we examined whether this virus could replicate in the tumor by staining adenovirus type 5 capsid proteins. Ad-*fos*ARE injected tumors showed capsid protein expressions and the abundance of the protein was higher in combination treatment than that of virus alone (Figure 3.9). These data indicate that Ad-*fos*ARE indeed replicated in tumors and PTX could activate it *in vivo*.

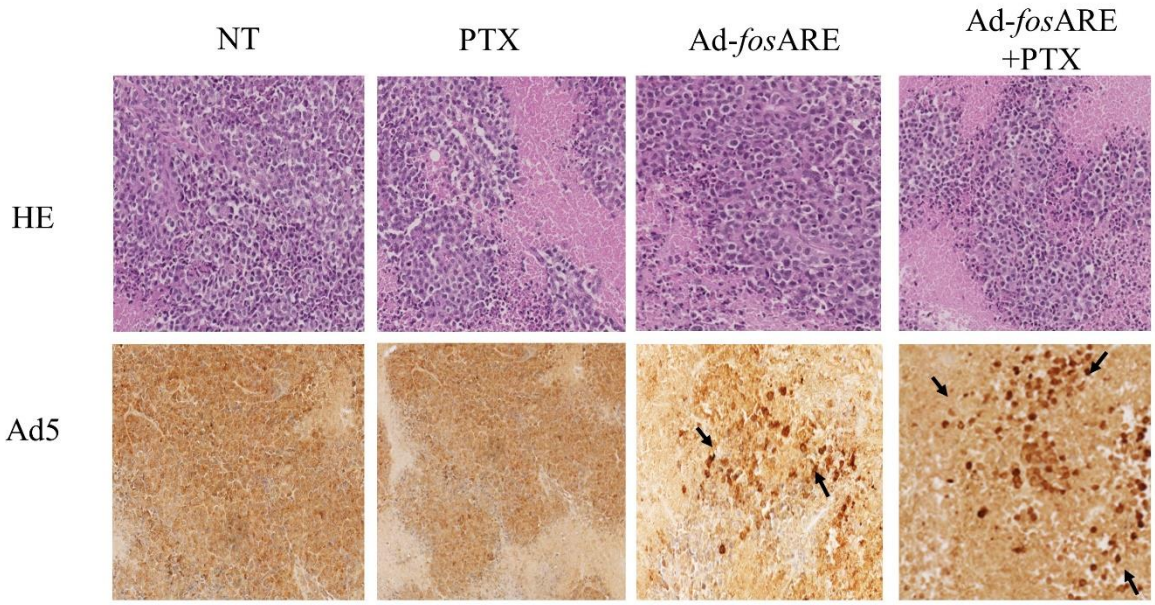

**Figure 3.9.** Effect of PTX on Ad-*fos*ARE propagation *in vivo*. HE and immunohistochemistry staining of HeLa tumors treated with Ad-*fos*ARE or PTX. Adenovirus detection (brown precipitations indicate by arrow) was performed by immunostaining using anti-adenovirus capsid antibody in all viruses injected tumors. NT indicates no treat**.**

### 3.4. Discussion

Antitumor activity of oncolytic adenoviruses can be enhanched when combined with chemotherapy or radiotherapy. In this study, we focused on the synergistic effect of Ad-*fos*ARE and PTX. In our previous project, we assessed the potentiality of Ad-*fos*ARE, furthermore, to overcome the limitation of an oncolytic virus as a standalone therapy, the combination of oncolytic virus and the chemotherapeutic agent was investigated. This approach was explored to see whether the two treatment modalities enhanced or synergized the effects of each other. Our results showed that PTX treatment synergistically increased the oncolytic activity of Ad-*fos*ARE both *in vitro* and *in vivo*. To the best of our knowledge, this is the first study to show that PTX activates oncolytic adenovirus function by promoting HuR cytoplasmic translocation.

Some studies demonstrated that nucleo-cytoplasmic HuR shuttling could utilize either the actin- or microtubules (MT)-dependent cytoskeleton for the transport of mRNA cargo(Cheng et al., 2013; Eberhardt et al., 2016; Doller et al., 2013). In our previous study, we reported that in cancer cells, HuR can translocate to the cytoplasm in an actin-independent manner but is actin-dependent in normal cells (Habiba et al., 2018). Although direct interaction between microtubules and HuR has not been demonstrated, it is speculated to be mediated by p38 mitogen-activated (MAP) kinase (Eberhardt et al., 2016; Fujiwara et al., 2011). PTX polymerizes and stabilizes the MT and arrests the cell cycle in G2+M phase and can increase the HuR mediated mRNA stabilization (Eberhardt et al., 2016; Subbaramaiah et al., 2003: Kotta-Loizou et al., 2016).In our study, HuR export was induced in cancer cells in the presence of PTX, while it decreased in normal cells, possibly due to the altered MT dynamics. In normal cells, PTX at a concentration of 1 μM directed the cells towards G2+M phase arrest, but in cancer cells, the cytotoxic effect could be observed at a concentration as low as 0.01–0.05 μM (Matsuoka et al.,1994; Cordes et al., 1998). In this study, we used 4 nM PTX; thus, the proliferation of Ad-*fos*ARE could be activated more due to the stabilization of ARE-mRNA. In previous studies, the combination of oncolytic virus and PTX were used with a focus on the synergism between mitotic arrest and apoptosis (Ingemarsdotter et al., 2010; Lin et al., 2008). In contrast, in the present study, we focused on cytoplasmic HuR translocation and stabilization of mRNA. This feature is unlikely to be observed in other oncolytic viruses, due to considerable unique advantages of Ad-*fos*ARE. Since many types of cancer cells have been reported to

stabilize ARE-mRNA (Khabar et al., 2017; Wang et al., 2013). Ad-*fos*ARE may be clinically relevant for the treatment of various cancers.

We also investigated the effect of PTX in E1A mRNA stabilization. After treatment with PTX, the half-life of E1A mRNA was increased, and these results indicate that Ad-*fos*ARE grows in an ARE-mRNA stabilization-dependent manner, thus increasing the level of cytoplasmic HuR in cancer cells by PTX enhances the oncolytic activity of Ad-*fos*ARE.

After adenovirus internalization into the host cells through viral receptors, MTs extending towards cell periphery usually encounter the virus, and the associated dynein motors bind them to MTs. Adenovirus-infection increased the post-translationally modified MTs through upregulated Glu-MTs and acetylated MTs through the RhoA-dependent mechanism, which favors viral delivery to the nucleus (Warren 2006). In this study, we showed that PTX upregulated the MT stabilization by utilizing the acetylated α-tubulin. We found that the levels of post-translationally modified MTs were increased after 1 h of treatment with PTX, and the levels were even higher with the combination of Ad-*fos*ARE and PTX. The ability to change the MTs dynamics of the host cells is the other advantage of the combinatorial treatment with PTX. Hence, PTX significantly influences the replication and spread of Ad-*fos*ARE, and additionally, the virus may also enhance the antitumor activity of PTX through the modification of MTs.

In the present study, we have shown that PTX synergizes with Ad-*fos*ARE by increasing the cytoplasmic HuR export, and, as shown previously, upregulating CAR and altering MTs dynamic instability. These findings indicate that PTX aids this oncolytic adenovirus engineered with ARE in multiple ways.

## 4. Conclusion and Future prospects

We found that a conditionally replicative adenovirus Ad-*fos*ARE is a potential oncolytic virus. In combination with PTX, the virus had a synergistic effect for cancer cells both *in vitro* and *in vivo*. PTX synergized with Ad-*fos*ARE by increasing the cytoplasmic HuR export, upregulating CAR and altering MTs dynamic instability. These findings indicate that PTX aids this oncolytic adenovirus in multiple ways.

Since Ad-*fos*ARE and PTX combined therapy is a safe and effective method, this synergism would be promising gene therapy for a patient with cancer, which can minimize the burden of chemotherapy. It is necessary to consider whether Ad-*fos*ARE will be effective against PTX-resistant cancer in the future.

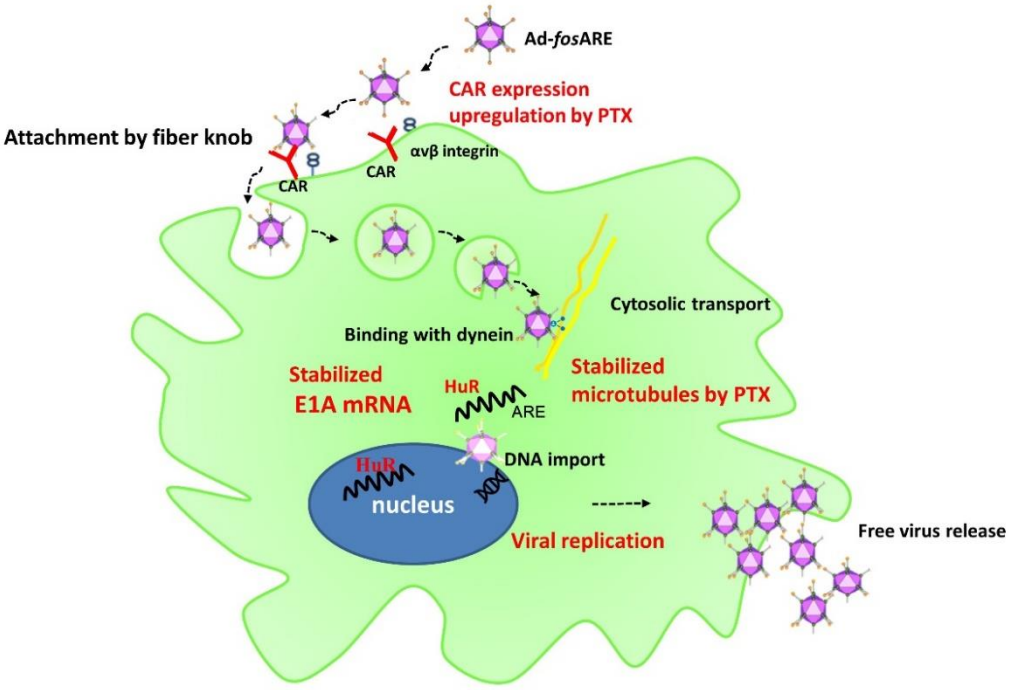


**Figure 3.10.** Diagramatic summary of the study

Acknowledgment

First of all, I would like to praise and thank almighty Allah, for his grace in accomplishing my Doctoral course timely.

I want to express my sincere gratitude to my supervisor Dr. Fumihiro Higashino, Associate Professor, Department of Molecular Oncology, Graduate School of Biomedical Science and Engineering affiliated with Department of Vascular Biology and Molecular Pathology, Faculty of Dental Medicine, Hokkaido University for his support for the course of my PhD and for giving me the opportunity to work with him. I always admire your optimism, enthusiasm and determination.

I would like to thank Dr. Hiroki Shirato, Dean of the Graduate School of Biomedical Science and Engineering, Hokkaido University, Japan for accepting me as his student.

I am sincerely grateful to my post-doc supervisor, Umma Habiba, for being such a competent mentor. This work would not have been possible to do without your good company. Thank you for being there for me even after changing your position and department.

I also want to deeply thank my other supervisor Aya Yanagawa all your help with experiments and expertise in so many laboratory techniques and providing advice for my projects.

I am grateful to Professor Dr. Kyoko Hida, Dr. Tetsuya Kitamura and Dr. Nako Maisi for your discussions and suggestion regarding my work.

I owe a lot of my personal development to my lab mates and friends. They made my journey easy and enjoyable and influenced my thought. I am thankfull to our lab staff Sanae Fukuda for always helping me out.

I am grateful to Bangabandhu Science & Technology Fellowship Trust, Ministry of Science and Technology of Bangladesh, for the grant of my Ph.D. fellowship.

I would like to express my gratitude to my parents and family who supported my ambition to pursue higher education and encouraged me to shine in both my professional and personal life. I am blessed to have such a loving and caring family. This includes my husband, Arefin Alam, whose emotional support and pragmatism have helped me get through difficult times and my daughter Feyha, who is my inspiration and hope. The result of my work reflected this thesis a reflection of all the encouraging people in my life, both professional and personal, who have drawn a security net that made it impossible for me to fail.

Thank you.

**References**

Abdelmohsen K, Srikantan S, Yang X, Lal, A., Kim, H.H., Kuwano, Y., Galban, S., Becker, K.G., Kamara, D., Cabo, R. and Gorospe, M.(2009). Ubiquitin-mediated proteolysis of HuR by heat shock. EMBO J. 28(9):1271–1282. doi:10.1038/emboj.2009.67

Abdolazimi, Y., Mojarrad, M., Pedram, M., Modarressi, M.H.(2007). Analysis of the expression of coxsackievirus and adenovirus receptor in fve colon cancer cell lines. World J. Gastroenterol. 13 (47), 6365-69. DOI:10.3748/wjg.v13.i47.6365

Abou El Hassan, M.A., Van der Meulen-Muileman I., Abbas, S., Kruyt, F.A. (2004). Conditionally replicating adenoviruses kill tumor cells via a basic apoptotic machinery – independent mechanism that resembles necrosis-like programmed cell death. J. Virol. 78(22), 12243-51. DOI: 10.1128/JVI.78.22.12243-12251.2004

Abudoureyimu, M., Lai, Y., Tian, C., Wang, T., Wang, R. and Chu, X. (2019) Oncolytic Adenovirus-A Nova for Gene-Targeted Oncolytic Viral Therapy in HCC. Front Oncol. 9:1182. doi:10.3389/fonc.2019.01182

Ahmed, A., Thompson, J., Emiliusen, L., Murphy, S., Beauchamp, R.D., Suzuki, K. A. (2003). Conditionally replicating adenovirus targeted to tumor cells through activated RAS/P-MAPK-selective mRNA stabilization. Nat. Biotech. 21, 771-777.

Alemany, R., Balague, C. and Curiel, D.T. (2000). Replicative adenoviruses for cancer therapy. Nat. Biotechnol. 18, 723–727. DOI:10.1038/77283

Anand, P., Kunnumakkara, A.B., Sundaram, C., Harikumar, K.B., Tharakan, S.T., Lai. O.S., Sung, B. and Aggarwal, B.B. (2008). Cancer is a preventable disease that requires major lifestyle changes. Pharmaceutical Research. 25 (9), 2097–116. *doi*:*10.1007/s11095-008-9661-*

Anke, T., Marcus, M., François, P.D., Frank, M., Hans-Georg, K., Andre, S., Andrea, M., and Hubert, L. (2019). Poly (ADP-Ribose) Polymerase-1 (PARP1) Deficiency and Pharmacological Inhibition by Pirenzepine Protects From Cisplatin. Front. Cell. Neurosci.13,104. https://doi.org/10.3389/fncel.2019.00406

Badawi, A., Biyanee, A., Nasrullah, U., Winslow, S., Schmid, T., Pfeilschifter, J. and Eberhardt, W. (2018). Inhibition of IRES-dependent translation of caspase-2 by HuR

confers chemotherapeutic drug resistance in colon carcinoma cells. Oncotarget. 9(26), 18367-18385. DOI:10.18632/oncotarget.24840

Bergelson, J.M., Cunningham, J.A., Droguett, G., Kurt-Jones, E.A., Krithivas, A., Hong, J.S., Horwitz, M.S., Crowell, R.L. and Finberg, R.W. (1997). Isolation of a common receptor for Coxsackie B viruses and adenoviruses 2 and 5. Science. 275, 1320-1323. DOI:10.1126/science.275.5304.1320

Berk, A.J. (2006). Adenoviridae: the viruse and their replication, Fields virology, In: HowleyDMKP ed. (Lippincott Williams & Wilkins, Philadelphia), pp 2354-2394.

Bischoff, J.R., Kirn, D.H., Williams, A., Heise, C., Horn, S., Muna, M., Ng, L., Nye, J.A., Sampson-Johannes, A., Fattaey, A. and McCormick, F. (1996). An adenovirus mutant that replicates selectively in p53-defcient human tumor cells. *Science*. 274, 373-376. DOI:10.1126/science.274.5286.373

Blower, M.D. (2013). Molecular insights into intracellular RNA localization. *Int. Rev. Cell.* Mol. Biol. 302, 1–39. DOI:10.1016/B978-0-12-407699-0.00001-7

Brennan, C.M. and Steitz, J.A.(2001). HuR and mRNA stability. Cell. Mol. Life Sci. 58, 266–277. DOI: 10.1007/PL00000854

Chen, C.Y. and Shyu, A.B.(1995). AU-rich elements: characterization and importance in mRNA degradation. Trends. Trends Biochem. Sci. 20, 465-470. DOI:10.1016/s0968-0004(00)89102-1

Cheng, Y.C., Liou, J.P., Kuo, C.C., Lai, W.Y., Shih, K.H., Chang, C.Y., Pan, W.Y., Tseng, J.T., and Chang, J.Y.(2013). MPT0B098, a novel microtubule inhibitor that destabilizes the hypoxia-inducible factor-1α mRNA through decreasing nuclear-cytoplasmic translocation of RNA-binding protein HuR. Mol. Cancer Ther.12, 1202–1212. DOI:10.1158/1535-7163.MCT-12-0778

Chou, C.T.(2010). Drug Combination Studies and Their Synergy Quantification Using the Chou-Talalay Method. Cancer res. 70(2). DOI:10.1158/0008-5472.CAN-09-1947

Cohen, S, Murphy, M.L.M., and Prather, A.A. (2019). *Ten Surprising Facts About Stressful Life Events and Disease Risk*. Annual Review of Psychology. **70**: 577–597. doi:10.1146/annurev-psych-010418-102857

Cordes, N., and Plasswilm, L.(1998).Cell line and schedule-dependent cytotoxicity of paclitaxel (Taxol): Role of the solvent Cremophor EL/ethanol. *Anticancer Res*. **1998**,

*18*, 1851–18577.

Davis, C.P. (2020).Cancer. Available at:https://www.medicinenet.com/cancer/article.htm (Accessed: 12th May 2020).

Debbas, M. and White, E. (1993). *Wild-type p53 mediates apoptosis by E1A, which is inhibited by E1B*. Genes & Development. **7** (4): 546–554. *doi*:*10.1101/gad.7.4.546*

DeMaria, C.T. and Brewer, G.(1996). AUF1 binding affinity to A+U-rich elements correlates with rapid mRNA degradation. J. Biol. Chem. 271, 12179-12184. DOI:10.1074/jbc.271.21.12179

Doller, A., Akool, el-S., Huwiler, A., Müller, R., Radeke, H.H., Pfeilschifter, J. and Eberhardt, W.(2008) Posttranslational modification of the AU-rich element binding protein HuR by protein kinase Cdelta elicits angiotensin II-induced stabilization and nuclear export of cyclooxygenase 2 mRNA. Mol. Cell. Biol.28, 2608–2625. DOI:10.1128/MCB.01530-07

Doller, A., Schulz, S., Pfeilschifter, J. and Eberhardt, W.(2013). RNA-dependent association with myosin IIA promotes F-actin-guided trafficking of the ELAV-like protein HuR to polysomes. Nucleic Acids Res. 41, 9152–9167, doi:10.1093/nar/gkt663.

Donnelly, O.G., Errington-Mais, F., Prestwich, R., Harrington, K., Pandha, H., Vile, R., and Melcher, A.A.( 2012). Recent clinical experience with oncolytic viruses. Current Pharmaceutical Biotechnology. 13 (9), 1834–41. *doi*:*10.2174/138920112800958904*

Eberhardt, W., Badawi, A., Biyanee, A., and Pfeilschifter, J.(2016). Cytoskeleton-Dependent Transport as a Potential Target for Interfering with Post-transcriptional HuR mRNA Regulons. Front. Pharmacol. 7, 251. DOI: 10.3389/fphar.2016.00251

Espel, E.(2005). The Role of the AU-rich Elements of mRNAs in Controlling translation. Semin. Cell. Dev. Biol.16, 59–67. DOI:10.1016/j.semcdb.2004.11.008

Fan, X.C. and Steitz, J.A.(1998). HNS, a nuclear-cytoplasmic shuttling sequence in HuR. Proc. Natl. Acad .Sci. 95, 15293–15298. DOI:10.1073/pnas.95.26.15293

Fok, P.T., Huang, K.C., Holland, P.C. and Nalbantoglu, J.(2007). The Coxsackie and Adenovirus Receptor Binds Microtubules and Plays a Role in Cell Migration. J. Biol. Chem. 282(10), 7512-21. DOI:10.1074/jbc.M607230200

Fu, L.Q., Wang, S.B., Cai. M.H., Wang, X.J., Chen, J.Y., Tong, X.M., Chen, X.Y. and

Mou, X.Z.(2019). Recent advances in oncolytic virus-based cancer therapy.Virus Research. 270:197675. doi: 10.1016/j.virusres.2019.197675

Fujiwara, Y., Kasashima, K., Saito, K., Fukuda, M., Fukao, A., Sasano, Y., Inoue, K., Fujiwara, T., and Sakamoto, H.(2011). Microtubule association of a neuronal RNA-binding protein HuD through its binding to the light chain of MAP1B. Biochimie. *93*, 817–822, doi:10.1016/j.biochi.2011.01.008.

Gene Therapy Review (2020). An Introduction to Cancer Gene Therapy, Available at: http://www.genetherapyreview.com/disease-targets/cancer/an-introduction-to-cancer-gene-therapy (Accessed: 3rd April 2020)

Habiba, U., Kitamura, T., Yanagawa-Matsuda, A., Higashino, F., Hida, K., Totsuka, Y. and Shindoh, M.(2016). HuR and podoplanin expression is associated with a high risk of malignant transformation in patients with oral preneoplastic lesion. Oncol. Lett. 5(12), 3199–3207. doi: 10.3892/ol.2016.5061

Habiba, U., Kuroshima, T., Yanagawa-Matsuda, A., Kitamura, T., Chowdhury, A., Jehung, J.P., Hossain, E., Sano, H., Kitagawa, Y., Shindoh, M. et al. (2018). HuR translocation to the cytoplasm of cancer cells in actin-independent manner. Exp. Cell Res. 369, 218–225, doi:10.1016/j.yexcr.2018.05.021.

Hao, J., Xie, W., Li, H., and Li, R.(2019). Prostate cancer-specific of DD3-driven oncolytic virus-harboring mK5 gene. Open Med. Wars. (Wars) 14, 1–9.

Heise, C., Sampson-Johannes, A., Williams, A., Mccormick, F., Von Hoff, D.D., and Kirn, D.H.(1997). Onyx-015, an E1B gene-attenuated adenovirus, causes tumor-specific cytolysis and antitumoral efficacy that can be augmented by standard chemotherapeutic agents. Nat. Med. 3, 639–645.

Holt, C.E., and Bullock, S.L.(2009). Subcellular mRNA localization in animal cells and why it matters. Science. 326, 1212–1216. DOI:10.1126/science.1176488

Horwitz, S.B.(1992). Mechanism of action of Taxol. Trends Pharmacol. Sci.13, 134-136. DOI:10.1016/0165-6147(92)90048-b

Ingemarsdotter, C.K., Baird, S.K., Connell, C.M., Öberg, D., Halldén, G. and McNeish, I.A.(2010). Low-dose paclitaxel synergizes with oncolytic adenoviruses via mitotic slippage and apoptosis in ovarian cancer. Oncogene. 29, 6051–606. DOI:10.1038/onc.2010.335

Islami, F., Goding Sauer, A., Miller, K.D., Siegel, R.L., Fedewa, S.A., Jacobs, E.J., McCullough, M.L., Patel, A.V., Ma, J., Soerjomataram, I., Flanders, W.D. et al. (2018). Proportion and number of cancer cases and deaths attributable to potentially modifiable risk factors in the United States. *CA Cancer J Clin*. 68 (1): 31–54. *doi*:*10.3322/caac.21440*. *PMID* *29160902*.

Jehung, J.P., Kitamura, T., Matsuda, A.Y., Kuroshima, T., Alam, M.T., Yasuda, M., Sano, H., Kitagawa, Y., Minowa, K., Shindho, M. and Higashino, F.(2018). Adenovirus infection induces HuR relocalization to facilitate virus replication. BBRC. 495(2),1795-1800. DOI: 10.1016/j.bbrc.2017.12.036.

Jenner, A.L., Yun, C.O., Kim, P.S., and Coster, A.C.F. (2018). Mathematical modelling of the interaction between Cancer cells and an oncolytic virus: insights into the effects of treatment protocols. Bull. Math. Biol. 80 (6), 1615–1629.

Kasuya, H., Takeda, S., Nomoto, S., and Nakao, A.(2005). The potential of oncolytic virus therapy for pancreatic cancer. Cancer gene ther. 2005, 12, 725–736. DOI: 10.1038/sj.cgt.7700830

Kelkar, S.A., Pfister, K.K., Crystal, R.G., and Leopold, P.L.(2004). Cytoplasmic dynein mediates adenovirus binding to microtubules. J. Virol.78(18), 10122–10132. DOI:10.1128/JVI.78.18.10122-10132.2004

Khabar, K.S. (2017). Hallmarks of cancer and AU-rich elements. Wiley Interdiscip Rev. RNA. 8, e1368, doi:10.1002/wrna.1368.

Kirn, D.(2000). Replication-selective Oncolytic Adenoviruses: Virotherapy aimed at genetic targets in cancer. Oncogene. 19, 6660–6669. DOI:10.1038/sj.onc.1204094

Knipe, D.M. and Howley, P.M. (2001). Fundamental Virology, 4th edn., Philadelphia, USA: Lippincott Williams & Wilkins. 1054

Kotta-Loizou, I., Vasilopoulos, S.N., Coutts, R.H., and Theocharis, S.(2016). Current Evidence and Future Perspectives on HuR and Breast Cancer Development, Prognosis, and Treatment. Neoplasia. 18, 674–688, doi:10.1016/j.neo.2016.09.002.

Kuroshima, T., Aoyagi, M., Yasuda, M., Kitamura, T., Jehung, J. P., Ishikawa, M., Kitagawa, Y., Higashino, F. (2011). Viral mediated stabilization of AU-rich element containing mRNA contributes to cell transformation. Oncogene. 30, 2912-2920.

Kruys, V., Marinx, O., Shaw, G., Deschamps, J., and Huez, G.(1989). Translational

blockade imposed by cytokine-derived UA-rich sequences. Science. 245, 852–5. DOI: https://doi.org/10.1126/science.2672333

Kruys, V., Wathelet, M., Poupart, P., Contreras, R., Fiers, W., Content, J., and Huez, G.(1987).The 3 untranslated region of the human interferon-beta mRNA has an inhibitory effect on translation. Proc. Natl. Acad. Sci. U.S.A. 84, 6030–4. DOI:10.1073/pnas.84.17.6030

Leopold, P.L., and Crystal, R.G.(2007). Intracellular trafficking of adenovirus: many means to many ends. Adv. Drug Deliv. Rev. 59, 810–821. DOI:10.1016/j.addr.2007.06.007

Lin, S.F., Gao, S.P., Price, D.L., Li, S., Chou, T.C., Singh, P., Huang, Y.Y., Fong, Y., and Wong, R.J.(2008). Synergy of a herpes oncolytic virus and paclitaxel for anaplastic thyroid cancer. Clin. Cancer Res. 14, 1519–1528, doi:10.1158/1078-0432.CCR-07-4628.

López de Silanes, I., Fan, J., Yang, X., Zonderman, AB., Potapova, O., Pizer, E.S., and Gorospe, M.(2003). Role of the RNA-binding protein HuR in colon carcinogenesis. Oncogene 22: 7146-7154.

Matsuoka, H., Furusawa, M., Tomoda, H., and Seo, Y. (1994). Difference in cytotoxicity of paclitaxel against neoplastic and normal cells. Anticancer Res. 14, 163–167.

McGuire, W.P., Hoskins, W.J., Brady, M.F., Kucera, P.R., Partridge, E.E., Look, K.Y., Clarke-Pearson, D.L., and Davidson, M.(1996). Cyclophosphamide and cisplatin compared with paclitaxel and cisplatin in patients with stage III and stage IV ovarian cancer. N. Engl. J. Med. 334, 1–6. DOI:10.1056/NEJM199601043340101

Nadar, M., Chan, M.Y., Huang, S.W., Huang, C.C., Tseng, J.T., and Tsai, C.H.(2011). HuR binding to AU-rich elements present in the 3’ untranslated region of Classical swine fever virus. Virol. J. 8, 340. DOI:10.1186/1743-422X-8-340

Goradel, N.H. N Mohajel, ZV Malekshahi, S Jahangiri, M Najafi, B Farhood, Keywan Mortezaee Babak Negahdari, Arash Arashkia. (2018). Oncolytic adenovirus: A tool for cancer therapy in combination with other therapeutic approaches.Journal of cellular physiology. 234 (6), 8636-8646. https://doi.org/10.1002/jcp.27850

Rowe, W. P., Huebner, R. J., Gilmore, L. K., Parrott, R. H., and Ward, T. G. (1953).

Isolation of a cytopathogenic agent from human adenoids undergoing spontaneous degeneration in tissue culture. Proceedings of the Society for Experimental Biology and Medicine, 84(3), 570–573.

Rux, J. J., and Burnett, R. M. (2004). Adenovirus structure. Human GeneTherapy, 15(12), 1167–1176.

Seidman, M.A., Hogan, S.M., Wendland, R.L., Worgall, S., Crystal, R.G., and Leopold, P.L.(2001). Variation in adenovirus receptor expression and adenovirus vector-mediated transgene expression at defined stages of the cell cycle. Mol. Ther. 4(1), 13-21. DOI:10.1006/mthe.2001.0414

*Silanes, I.L.,* Fan, J.; Yang, X.; Zonderman, A.B.; Potapova, O; Pizer, E.S. and Gorospe, M.(2003). Role of the RNA-binding protein HuR in colon carcinogenesis. Oncogene. 22: 7146-7154. https://doi.org/10.1038/sj.onc.1206862

*Silanes, I.L., Lal, A., and Gorospe, M.(2005). HuR: post-transcriptional paths to malignancy. RNA biology. 2, 11-3. https://doi.org/10.4161/rna.2.1.1552*

Subbaramaiah, K., Marmo, T.P., Dixon, D.A., and Dannenberg, A.J.(2003). Regulation of cyclooxgenase-2 mRNA stability by taxanes: evidence for involvement of p38, MAPKAPK-2, and HuR. J. Biol. Chem. *278*, 37637–37647, doi:10.1074/jbc.M301481200.

Taguchi, S., Fukuhara, H., and Todo, T. (2018). Oncolytic virus therapy in Japan: progress in clinical trials and future perspectives. Japanese Journal of Clinical Oncology. 49, 201–209.

Tazawa, H.; Kuroda, S.; Hasei, J.; Kagawa, S.; Fujiwara, T. Impact of Autophagy in Oncolytic Adenoviral Therapy for Cancer. *IJMS.* 2017 *18*, 1479. https://doi.org/10.3390/ijms18071479

Tomko, R.P.; Xu, R.; Philipson, L. HCAR and MCAR: the human and mouse cellular receptors for subgroup C adenoviruses and group B coxsackieviruses. *Proc. Natl. Acad. Sci. U.S.A.* 1997, 94, 3352-3356. DOI:10.1073/pnas.94.7.3352

Wang, J., Guo, Y., Chu, H., Guan, Y., Bi, J., and Wang, B.(2013). Multiple functions of the RNA-binding protein HuR in cancer progression, treatment responses and prognosis. Int. J. Mol. Sci. 14, 10015–10041, doi:10.3390/ijms140510015.

Wang, K.,Kievit, F.M., and Zhang, M. (2016). Nanoparticles for cancer gene therapy:

Recent advances, challenges, and strategies. Pharmacological Research, 114, 56-66.

Warren, J.C., Rutkowski, A. and Cassimeris, L. (2006). Infection with replication-deficient adenovirus induces changes in the dynamic instability of host cell microtubules. Mol. Biol. Cell. 17, 3557-68. DOI:10.1091/mbc.E05-09-0850

WHO. (2018). *Cancer,* Available at: *https://www.who.int/news-room/fact-sheets/detail/cancer* (Accessed: 12th May 2020).

WHO. (2020). Noncommunicable diseases. Available at: *https://www.who.int/health-topics/noncommunicable-diseases#tab=tab_1* (Accessed: 11th May 2020).

Yeh, C.H., Hung, L.Y., Hsu, C., Le, S.Y., Lee, P.T., Liao, W.L., Lin, Y.T., Chang, W.C., and Tseng, J.T.(2008). RNA-binding protein HuR interacts with thrombomodulin 5'untranslated region and represses internal ribosome entry sitemediated translation under IL-1 beta treatment. Mol. Biol. Cell. 19, 3812-3822. DOI:10.1091/mbc.e07-09-0962

Yu, D.C., Chen, Y., Dilley, J., Li, Y., Embry, M., Zhang, H., Nguyen, N. and Amin, P.(2001). Antitumor synergy of CV787, a prostate cancer-specific adenovirus, and paclitaxel and docetaxel. Cancer Res. 61, 517

# Supplementary Data

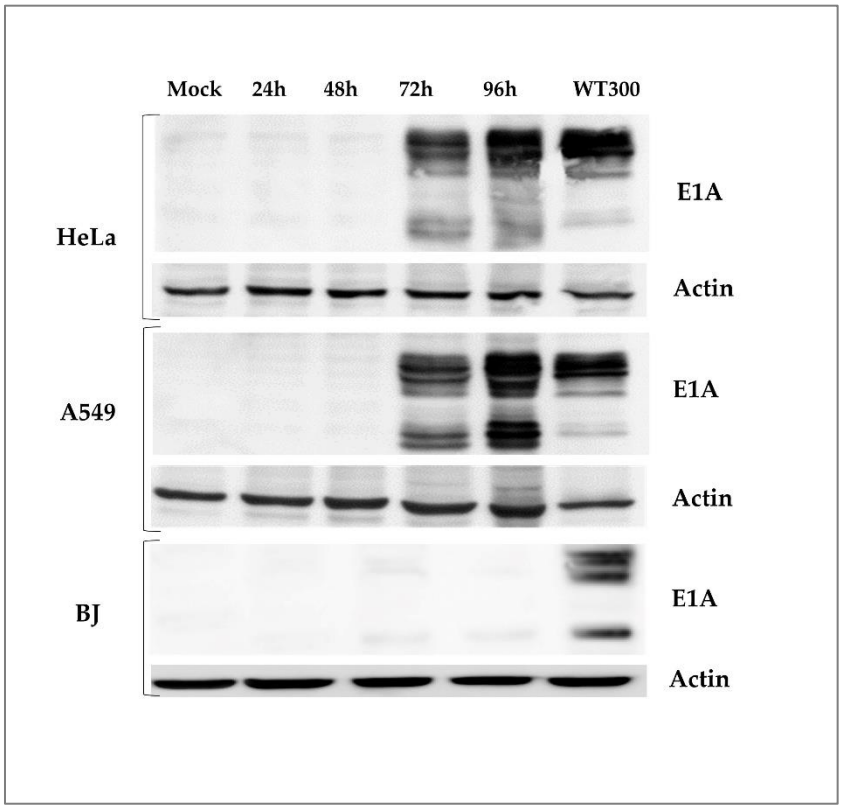


**Supplementary Figure 1.** Time course of expression of virus protein in Ad-*fos*ARE infected cells. A549, HeLa and BJ cells were infected with both viruses. The Ad-*fos*ARE virus was infected to cells for 24, 48, 72 and 96 h, and WT300 were infected to cells for 24h as a positive control. Total cell extracts were prepared, then the expression of early gene E1A and actin was estimated by western blot analysis.

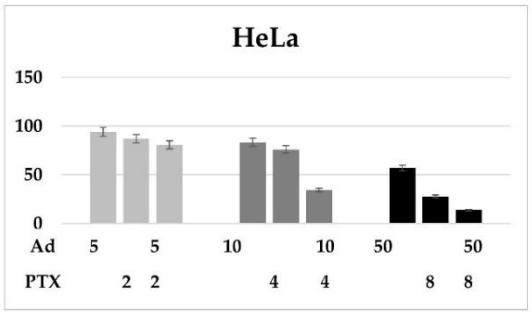


| Dose PTX nM | Ad-fosARE ifu/cell | Effect | CI |
|---|---|---|---|
| **2.0** | 5.0 | 0.6 | 0.67835 |
| **4.0** | 10.0 | 0.22 | 0.50583 |
| **8.0** | 50.0 | 0.13 | 0.85878 |

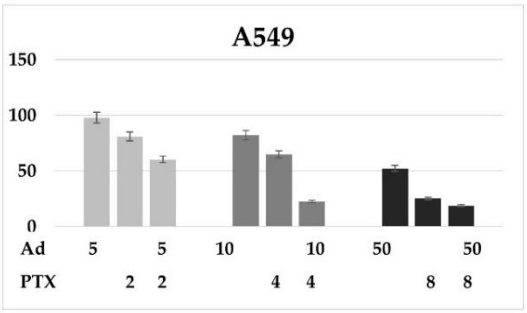


| Dose PTX nM | Ad-fosARE ifu/cell | Effect | CI |
|---|---|---|---|
| **8.0** | 50.0 | 0.81 | 0.97063 |
| **4.0** | 10.0 | 0.77 | 0.52767 |
| **2.0** | 5.0 | 0.6 | 0.40865 |

**Supplementary Figure 2.** Calculation of combination index for Ad-*fos*ARE and PTX. HeLa and A549 cells were transfected with 3 different dosages of Ad-*fos*ARE, PTX, and combination. CIs of Ad-*fos*ARE or PTX or in combination with were calculated using Compusyn and plotted against the percentage of cell death resulting from combined therapy. CI of <0.9 indicates synergy, CI between 0.9 and 1.1is addictive, and CI of >1.1indicates antagonism.

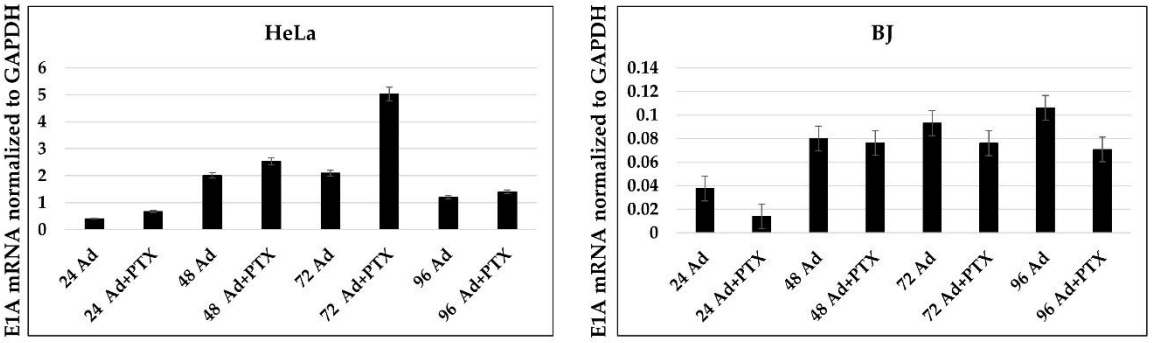


**Supplementary Figure 3.** E1A mRNA expression in Ad-*fos*ARE infected cells. HeLa and BJ cells were infected with Ad-*fos*ARE (MOI 10 ifu/cell) and combination with PTX (4 nM) for 24, 48, 72 and 96 h and the expression of E1A mRNA were determine using RT-PCR. Data shown as mean $\pm$ standard of three independent experiments.

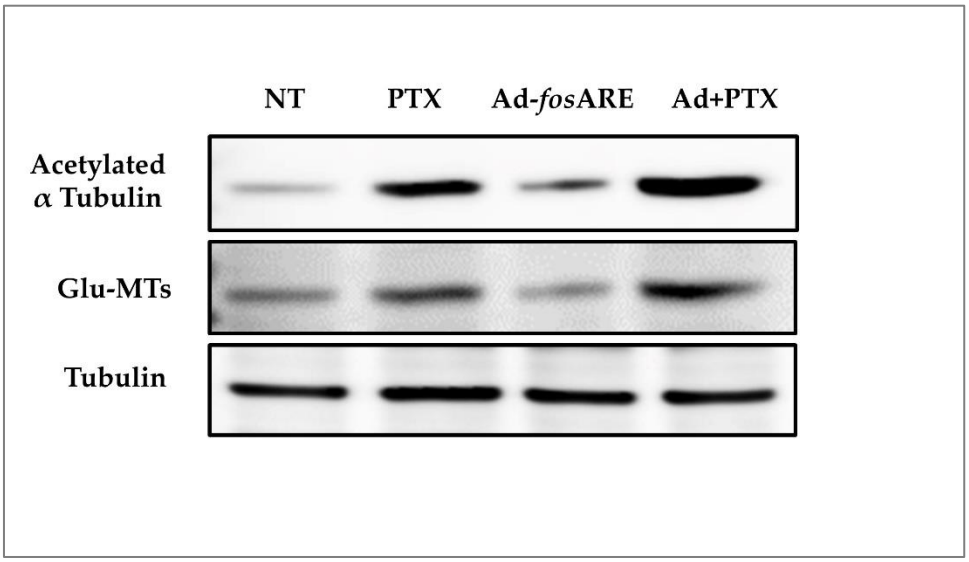


**Supplementary Figure 4.** Level of posttranslationally modified MTs after combination treatment. To determined posttranslationally modified tubulin, HeLa cells were treated with Ad-*fos*ARE, PTX and combination. The expression of acetylated and Glu-MTs was quantified by densitometry and the values were normalized to non-infected conditions.

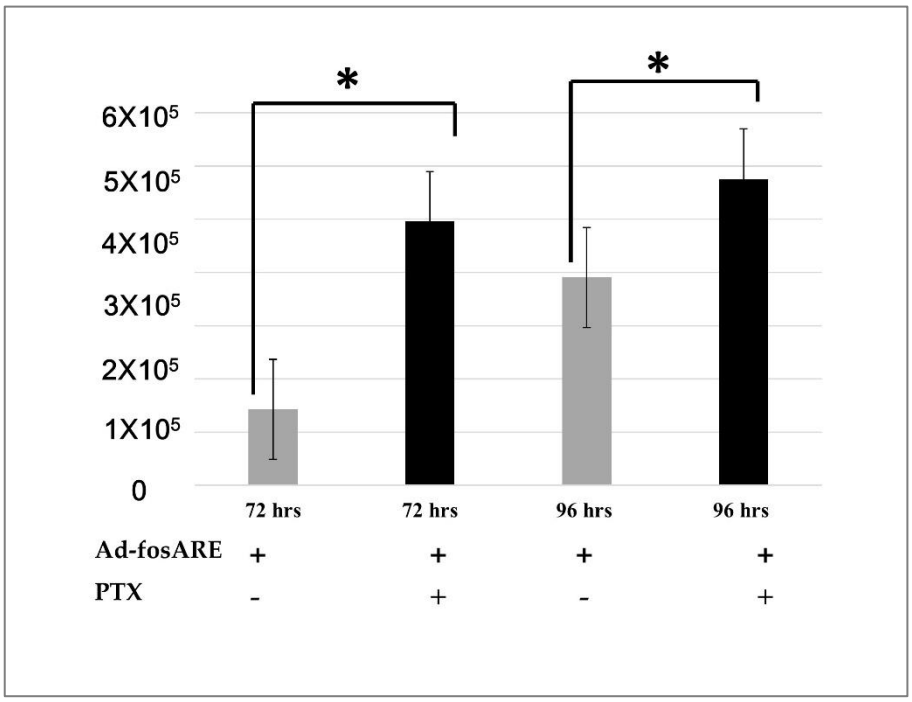


**Supplementary Figure 5.** Intracellular virus propagation after combination treatment. HeLa cells were treated with PTX and infected with 10 ifu/cell of Ad-*fos*ARE. Only the attached cells were tested for virus particles 72 and 96 h after infection with removing the supernatant. Data are shown above as the mean ± standard deviation of three independent experiments (* indicates $p < 0.05$).